Cretaceous Research 179 (2026) 106268

Contents lists available at ScienceDirect

Cretaceous Research

journal homepage: www.elsevier.com/locate/CretRes

Reptile footprints on a pelagic seafloor as a vestige of a synsedimentary seismic event in the lower Campanian Scaglia Rossa basin of the Umbria-Marche Apennines (Italy)

Paolo Sandroni [a], Nathan S. Church [b,*], Rodolfo Coccioni [c,d], Fabrizio Frontalini [e], Maurizio Mainiero [f], Alessandro Montanari [g]

[a] Centro Funzionale Multirischi Protezione Civile Regione Marche, Via del Colle Ameno, 5, Torrette, 60126 Ancona, Italy
[b] Department of Geosciences, Norwegian University of Science and Technology, 7031 Trondheim, Norway
[c] University of Urbino "Carlo Bo", 61029 Urbino, Italy
[d] Osservatorio Pianeta Terra, 60013 Corinaldo, Italy
[e] Department of Pure and Applied Sciences, University of Urbino "Carlo Bo", Crocicchia, 61029 Urbino, Italy
[f] Studio Geologico, Via XXIX Settembre 2/o, 60122 Ancona, Italy
[g] Osservatorio Geologico di Coldigioco, Cda. Coldigioco 4, 62021 Apiro, Italy

ARTICLE INFO

Article history:
Received 20 December 2024
Received in revised form
12 November 2025
Accepted in revised form 13 November 2025
Available online 19 November 2025

Keywords:
Northern Apennines
Monte Cònero
Scaglia Rossa
Early Campanian event
Vertebrate trace fossils

ABSTRACT

A group of free climbers by chance discovered a large number of footprint traces deeply impressed on a vast pelagic limestone slab on the steep northeastern limb of the Monte Cònero anticline, near the city of Ancona (Marche region of central-eastern Italy). The footprints probably represent a stampede of panicking sea turtles that were mobilized *en masse* by an earthquake. These tracks were subsequently covered by a fluxoturbidite triggered by the same earthquake. The same layer is exposed in a 40-m-thick section along the littoral zone below. This new section provides the ability, through combined bio- and magneto-stratigraphic analysis, to place the footprint layer in the lower Campanian foraminiferal bio-zone *Globotruncanita elevata* and the lowermost part of magnetochron C33n. Most of this section comprises calcarenitic and calcilutitic turbidites interbedded with pelagic biomicrites, which witnessed a period of enhanced seismic activity exacerbated by a climate change-driven eustatic sea level fluctuation. Following a review of the sedimentological and tectono-seismic history of the Cretaceous Umbria-Marche paleobasin with particular attention to the Monte Cònero area, we describe and document our integrated stratigraphic analysis of the new section exposed along the northeastern littoral known as La Vela Beach.

1. Introduction

1.1. The discovery

In the spring of 2019, a group of free climbers went on an explorative excursion around the steep northeast-facing slopes of Monte Cònero, the easternmost and most external anticline of the northern Apennine foreland thrust-and-fold belt (Fig. 1), which is located some 8 km south of the port city of Ancona (Marche region of Italy). This area is located along a littoral stretch of the Cònero Regional Park just south of the sea stack named "*La Vela*" (The Sail in English) (Fig. 1), the public access to which (including standing, transit, and docking) is today forbidden by the municipal authority due to frequent rock falls (Comune di Ancona, 2019). The intended plan of the climbers was to explore large flat rock surfaces discernible from offshore but not quite visible from the beach, which they referred to as "*Le Placche della Vela*" (The Sail Slabs in English) (Fig. 2A-B). The rock climbers immediately noticed a most unusual, dense series of traces on the surface of one of these rock slabs that recalled some marine tetrapod paddle prints discovered by Natali et al. (2019), and recently ascribed to the new ichnogenus and species *Coneroichnus marinus* by Natali and Leonardi (2023) in

* Corresponding author.
E-mail addresses: paolosandroni@gmail.com (P. Sandroni), nathan.church@ntnu.no (N.S. Church), rodolfo.coccioni@uniurb.it (R. Coccioni), fabrizio.frontalini@uniurb.it (F. Frontalini), info@studiogeologico.com (M. Mainiero), Sandro.coldigioco@gmail.com (A. Montanari).

https://doi.org/10.1016/j.cretres.2025.106268

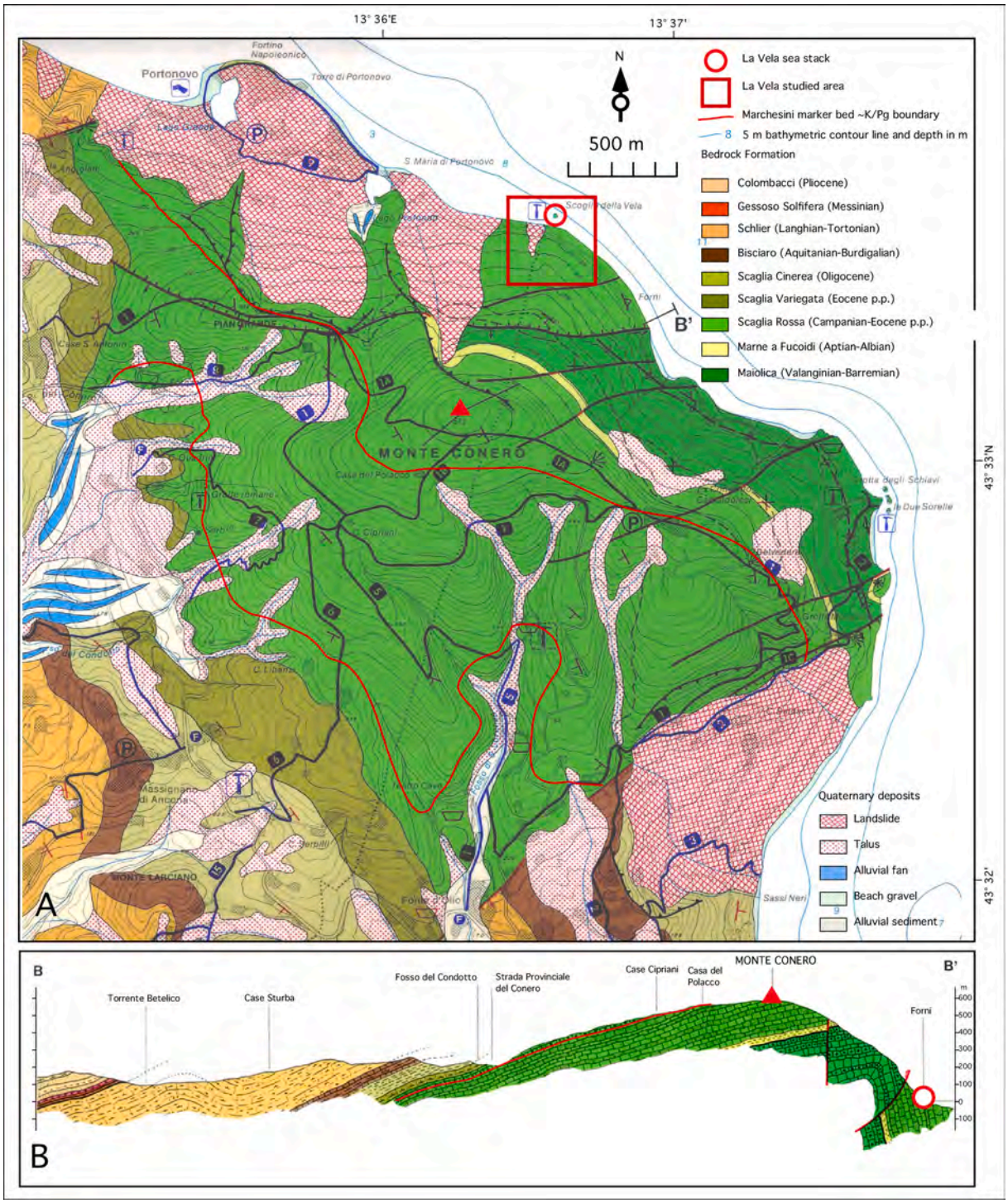

Fig. 1. A) Geologic map of Monte Cònero, with red line indicating the trace of the basal Danian Marchesini calcarenite marker bed (i.e., the Mega T; Montanari, 1979; Montanari & Koeberl, 2000), which is located at about 80 cm above the K/Pg boundary, and the studied area framed by a red square; B) Geologic cross section across the Cònero anticline B–B[1]. Geologic base map and cross section are from Coccioni (2022).

an outcrop of the Maiolica Formation in another prohibited area of the Cònero Park, the so-called "*Le Placche dei Gabbiani*" (The Seagull Slabs). Like the La Vela Slabs that overhang the eponymous beach, the Seagull Slabs overhang the picturesque Due Sorelle Beach on the easternmost point of the Cònero promontory (see Fig. 1A for location), which is yet not prohibited despite it too presenting a degree of geomorphologic precariousness (Angeli, 1999; see also Fig. 6 in Aringoli et al., 2014). The free climbers took digital pictures of these footprint-like traces and showed them to one of us (P.S.), who is also a free climber with a degree in Geology. P.S. later returned to the La Vela site in company with co-author M.M. to check the traces and to acquire digital photographs of the footprint-like features and fossil traces such as *Zoophycos* on different parts of the slab (Fig. 3A, B. C, and D). Using a small drone, they took pictures of bottom current marks on the surface of similar slabs exposed on sites 10 and 12 (Fig. 3E and F, respectively;

see Fig. 2A for location). On that occasion, P.S. and M.M. collected a few rock samples from a short section of limestone beds directly overlying the layer with the presumed footprints, which is exposed high up on Site 9 (see location in Fig. 2A).

1.2. Preliminary sedimentologic and stratigraphic assessments

After having inspected the photographs and analyzed the few samples collected from the logged section of Site 9 (Fig. 4A and B), thin-section and image analysis of polished slabs revealed that the layer with the footprints is a pelagic limestone containing tests of planktonic foraminifera suspended in a micritic matrix (Fig. 4C–E). Among others, the lowermost Campanian zonal biomarker *Globotruncanita elevata* was recognized in the same pelagic limestone sample CON-VEL 9.2 (Fig. 4C) at 1.05 m level in the lithostratigraphic log of Fig. 4A. Thin sections also revealed bioturbation traces, probably representing *Planolites* or *Zoophycos* burrows. By contrast, the polished surface of limestone sample CON-VEL 9.1 from meter level 1.10 in the log of Fig. 4A, which immediately overlies this footprint-studded pelagic limestone, exhibited internal structures such as cross-laminations and grading (Fig. 4D). Texturally, this limestone is essentially a grain-supported biomicrite mostly made of small planktonic foraminiferal tests and other rare biogenic carbonate clasts such as inoceramid prisms and calcispheres (Fig. 4G). However, fine textural and structural features such as grading, laminations, microfossils, bioturbation traces were not visible on a wetted surface of a hand sample looking through a canonical 10-x-magnification loupe lens. Hand samples appeared in the field as absolutely homogeneous, superfine limestones with a milky-white color (see insets in Fig. 4C and D). In short, we hypothesized that the footprints, which were probably made by a group of medium-sized marine vertebrates paddling towards southwest on a soft pelagic seafloor (Fig. 2B), were preserved on that oozy sediment because they were immediately buried and sealed under a calcilutitic turbidite (Fig. 4A).

1.3. Preliminary ichnopaleontologic assessments

A question that inevitably comes to mind is: what kind of animal(s) may have left those footprints? One first step in answering this legitimate question is to consider that in the Late Cretaceous the only vertebrates roaming the deep sea were fish and reptiles. Well-preserved skeletal fossils of these aquatic animals are occasionally found in pelagic limestones but they are never associated with their fin-, paddle-, or footprint traces. After all, fossil traces on the surface of an oozy seafloor cannot last long before they are obliterated by bottom currents and/or bioturbation. Moreso if one considers that the biomicritic pelagic sediment that yielded the Umbria-Marche (U-M) Scaglia Rossa limestone, which was continuously homogenized by synsedimentary bioturbation, was deposited at a mean accumulation rate in the order of ~10 m m.y.$^{-1}$ (i.e., 10 mm per thousand years; e.g., Arthur and Fischer, 1977; Lowrie et al., 1990; Mukhopadhyay et al., 2001; Bice et al., 2007; Gardin et al., 2012; Wendler, 2013; Husson et al., 2014; Sinnesael et al., 2016). For this reason, reports of fossil footprints on a seafloor of any geological age are rare in scientific literature (e.g., Zhang et al., 2014; Lockley et al., 2018; Natali et al., 2019; Baucon et al., 2023).

Excluding fish, which do not use their fins to paddle on the seafloor, for our lowermost Campanian case of Monte Cònero, we have to consider marine reptiles of three kinds: plesiosaurs (giant reptiles typically with a long neck and a small head), mosasaurs (i.e., large marine reptiles first found near the Meuse River [*Mosa* in Latin]; e.g., Lindgren et al., 2010), and sea turtles, specifically Protostegidae (e.g., Danilov et al., 2022; Serafini et al., 2024). While numerous remains of these Cretaceous marine reptiles were found in the Scaglia Rossa of the pre-Alpine Venetian region of northern Italy (Zorzin, 2016, 2017, 2022), no fossils of plesiosaurs or sea turtles were ever found in the U-M Scaglia Rossa pelagic limestone. Nevertheless, one well-preserved mosasaur tooth was reported by Montanari (1979) from the Via Flaminia section at Furlo in the Marche Apennine, which was extracted by quarry worker Mr. Elio Santi from a pink pelagic limestone bed some 19 m below the K/Pg boundary (Fig. S1), thus approximately corresponding to the base of mid-Maastrichtian magnetochron C30n (Alvarez and Lowrie, 1984; see also Fig. 5.7.6.12 on p. 238 in Montanari and Koeberl, 2000). Moreover, in 1982 Walter Alvarez found a rounded pebble of tholeiitic basalt embedded in a pink pelagic limestone layer of Maastrichtian Scaglia Rossa in the Furlo Upper Road section (Alvarez and Lowrie, 1984), which at first sight resembled a meteorite but was later interpreted as a gastrolith (Walter Alvarez, personal communication, November 2024), similar to those found among marine reptile remains in the Venetian Scaglia Rossa Fm (Gonzato and Ferrari, 2020; Serafini et al., 2024). In any case, all these marine reptiles used their paddle-like forelimbs as “freestyle” swimming propulsion. By contrast, extant sea turtles use both their fore and hind flippers, and sometimes their tail, to clumsily drag themselves onto dry sandy beaches to lay their eggs, leaving complex yet ephemeral traces similar to caterpillar tracks but with varying patterns and shapes according to the species. Lockley et al. (2019) reports on a case of such an on-land sea turtle tracks in a South African Pleistocene beach deposit.

However, one can only rely on imagination of how an extinct finned reptile may leave paddling tracks on a soft sediment seafloor. A rare if not unique case is given by a series of regular and symmetric paddle tracks left on a shallow seafloor by a Triassic nothosaur, which were studied and documented in detail by Zhang et al. (2014) (see synoptic Fig. 5A). As for sea turtles, the first report of swim tracks on a Campanian shallow water environment is by Lockley et al. (2018). Lockley and co-workers attributed regularly spaced traces, shown in Fig. 4 in their paper, to small turtles swimming near the seafloor all in the same direction, and not dragging their body onto it, as a female sea turtle would do on a dry sandy beach. Our synoptic Fig. 5B illustrates how a modern sea turtle swimming close to the seafloor might brush or even dip the tip of its fore flippers (and maybe also the tip of its tail) into the soft sediment, leaving regularly spaced parallel arcuate marks or irregular roundish pockmarks like those present on the surface of the La Vela Slabs (Fig. 3B-C).

To address the original question of what animal(s) may have left footprints on the oozy pelagic seafloor of the Campanian Scaglia Rossa at Monte Cònero, we consider that while plesiosaurs and mosasaurs were probably solitary predators and Late Cretaceous sea turtles were probably solitary prey like their modern relatives, female turtles of most of the seven extant species periodically gather in large herds to migrate towards tropical or temperate sandy beaches to lay their eggs. However, only the olive ridley (*Lepidochelys olivacea*) and Kemp's ridley (*Lepidochelys kempii*) sea turtles simultaneously land by the thousands on tropical sandy beaches to lay their eggs (e.g., Wibbels and Bevan, 2016, and references therein). Other species, such as the green sea turtle (*Chelonia mydas*), the loggerhead (*Caretta caretta*), and the giant leatherback (*Dermochelys coriacea*), undertake long-distance mass migrations, but they typically nest separately or in smaller groups on tropical or temperate sandy littorals. By contrast, large populations of herbivore species such as *Chelonia mydas*, constantly roam around shallow water coral reefs, where they find an abundant source of energy in seagrass and algae. Similarly, large numbers of principally predator species, such as

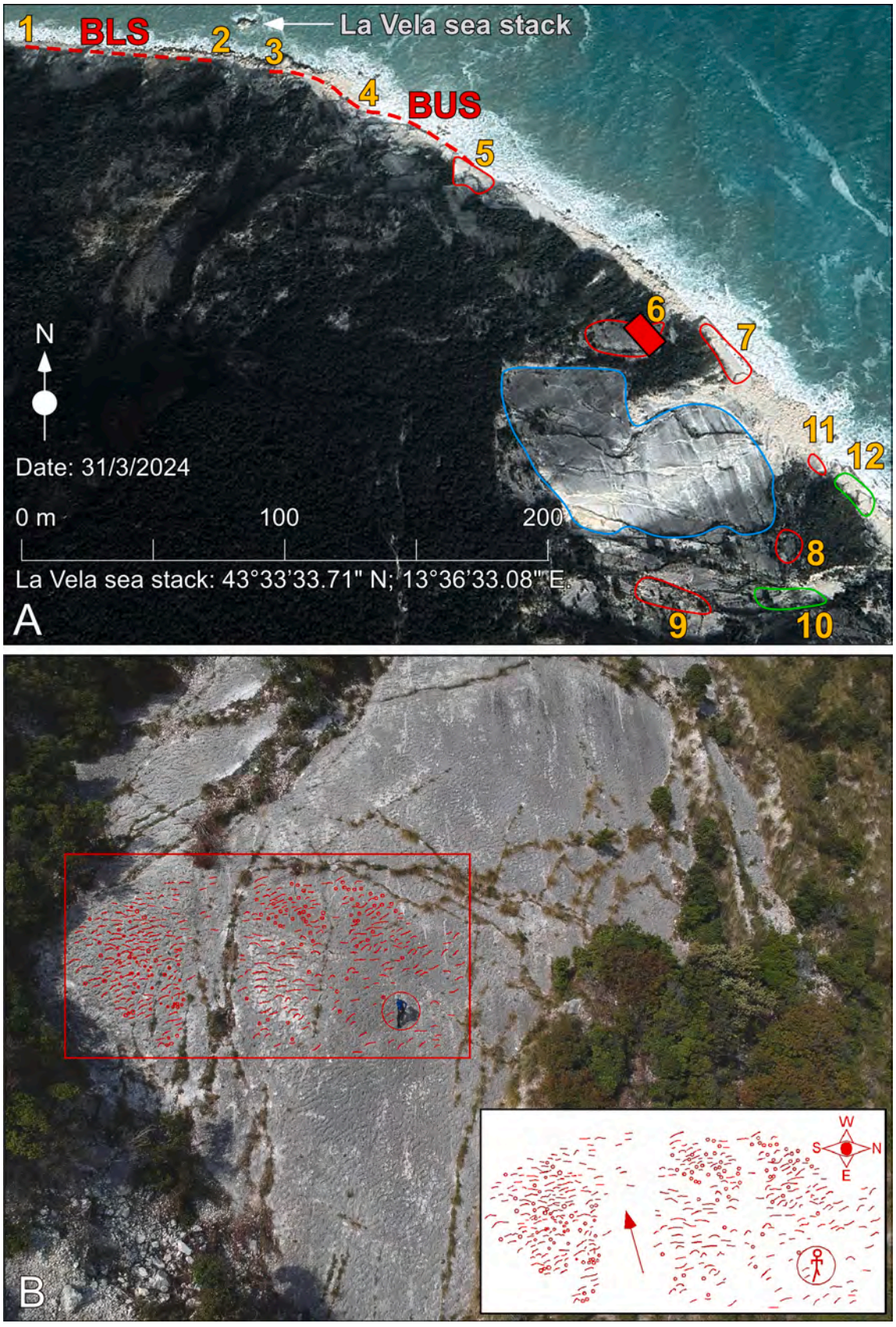

Fig. 2. A) Aerial image of the studied La Vela area on the steep northeastern limb of the Monte Cònero anticline (sea stack at top of image is located at 43°33′33.71″ N, 13°36′33.08″ E). Dashed red lines along the coast indicate measured and sampled stratigraphic sections, which are named Beach Lower Section (BLS), and Beach Upper Section (BUS). The yellow numbers indicate sites where the bedrock formations were inspected and measured along the beach (i.e., Sites 1 to 2 = Maiolica Fm.; Sites 3, 4, 5, 7, 11, and 12 = Scaglia Rossa Fm.). Sites 6, 8, 9, and 10 were surveyed and studied using high-resolution aerial (drone) digital photographs and ground truthing on foot using appropriate climbing gear

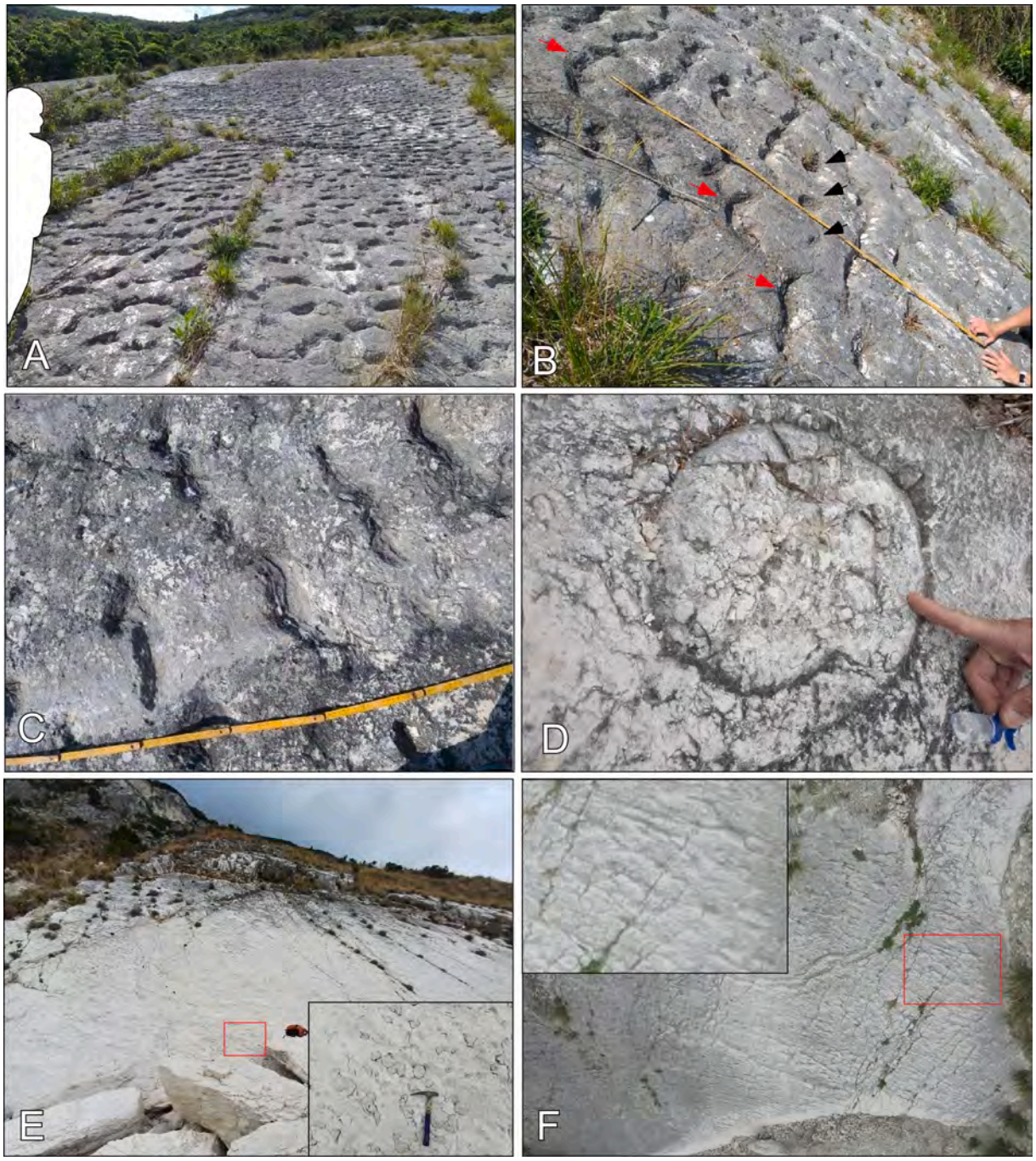

Fig. 3. A) Panoramic view of the limestone slab exposed on Site 6, showing the extension and density of footprint marks. Outline of a covert free climber for scale on the lower left foreground of the picture; B) Detail of the slab surface of Site 6 showing a random distribution of arched paddle print marks (red arrows), and round, cup-shaped print marks (black arrows); C) Close up photograph of regularly spaced double curved paddle print marks on the same slab surface of Site 6; D) A *Zoophycos* fossil trace on the surface of the same footprint bed exposed on Site 9; E) Panoramic view of the slab on Site 12. The top surface of this pelagic limestone bed is studded with flute marks filled with the beige sediment from the bottom of a now-removed overlying calcarenitic turbidite (see enlargement of the red rectangle area shown in the inset); F) Aerial (drone) photograph of the subvertical slab of Site 10. The surface of this limestone bed exhibits a dense series of elongated positive structures, which may represent current ripple marks (see them enlarged in the inset). In the center of this image, notice a long sinusoidal trace crossing the ripple set, which may represent a groove of an object dragged on the oozy seafloor by a bottom current.

and expertise. Areas contoured with a red line represent the exposed top surface of a pelagic limestone layer of the Campanian Scaglia Rossa Fm., studded with a myriad of footprints. The red rectangle on the slab of Site 6 (strike 315°NW; dip 45°NE), refers to the red rectangular frame area in Fig. 2B. The vast slab countered with a blue line represents the trace-free top surface of a pelagic limestone, which is found a few stratigraphic meters below the footprint layer. The slabs contoured with a green line represent the top surface of pelagic limestones found a few stratigraphic meters above the footprint layer exhibiting flute marks on Site 12, and probable ripple structures on Site 10 (see Fig. 3 E and F, respectively). B) Aerial orthogonal drone photograph of the slab of Site 6 (see red rectangle in Fig. 2A). The whole surface is studded with interpreted footprint traces, which have been marked with red lines and circles in the red rectangular, ~10 × 20-m area. Note in the inset diagram that arched traces suggest a general southwest progression (red arrow) when compared with fossil sea turtle paddle prints shown in figures 3A, 5 A-D, 7, and 9A in Lockley et al. (2019). See some details of these footprints in Fig. 3A, B, and C.

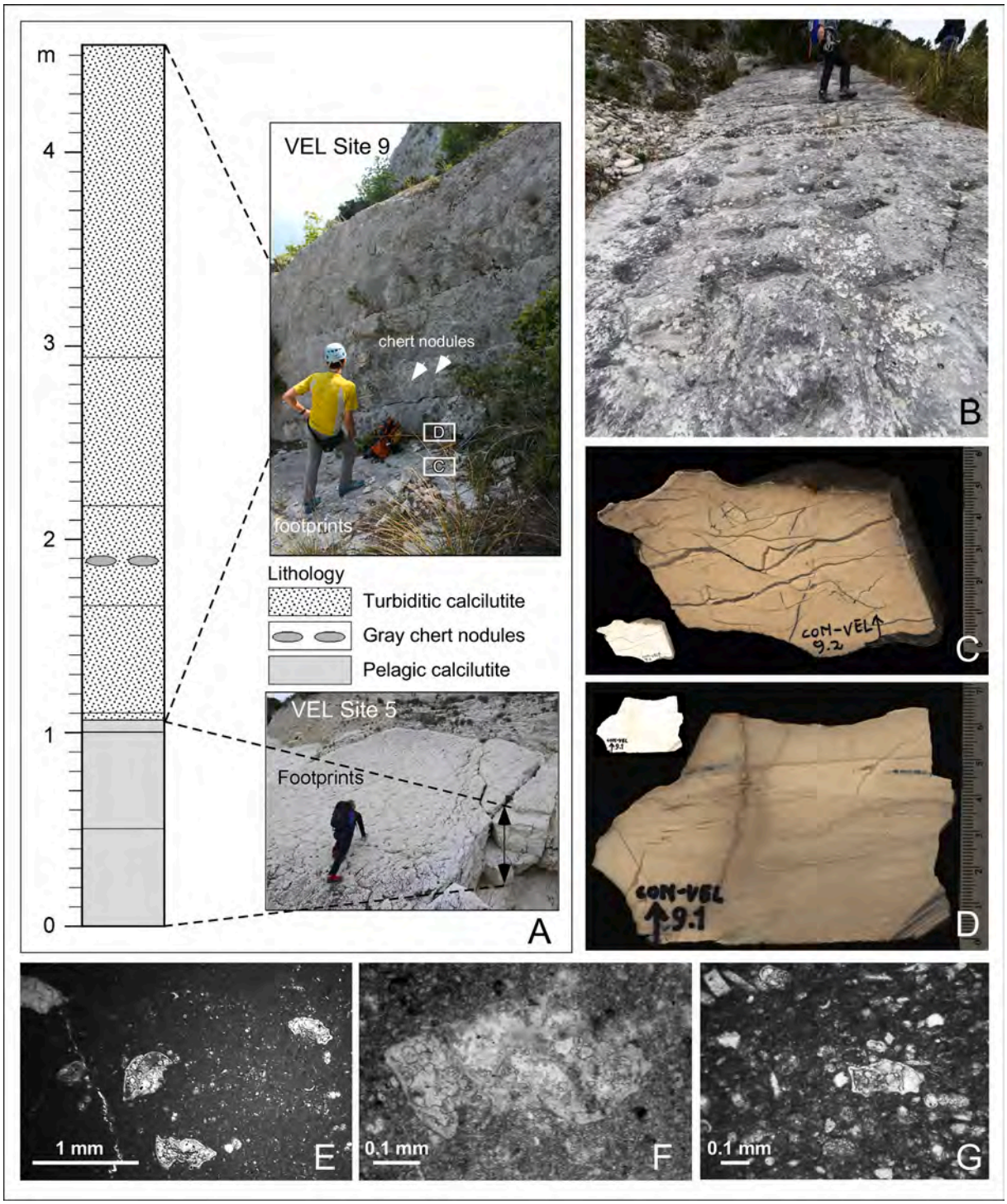

Fig. 4. A) Composite lithostratigraphy of the section exposed on Site 5 and Site 9; B) Panoramic photograph of the footprints slab exposed on Site 9; C) Polished slab of the footprint layer from meter level 1.05 in the section at Site 9. This image was obtained with a photo scanner at a resolution of 1600 dpi. Internal texture and sedimentary structures are not visible with the naked eye on a polished surface, which would appear white and completely homogeneous (see inset), but they become visible once the image is manipulated in Photoshop for luminosity (i.e., darkened) and enhanced contrast. In this case, the manipulated image does not show any internal sedimentary structure. Thin sections revealed that this calcilutitic limestone is a pelagite made up primarily of sparse planktonic foraminiferal tests suspended in a micritic matrix (see in E a thin section microphotograph of sample CON-VEL 9.2 at 1.05 m in the logged section of Site 9). Among them, the zonal marker *Globotruncanita elevata* is shown in F; D) Image of a polished slab of the limestone sample CON-VEL 9.1, collected from meter level 1.10 in the section at Site 9 (see microfacies in G). This calcilutitic detrital limestone rests on top of the footprints layer and in an enhanced digital image exhibits internal structures such as grading and microlaminations, suggesting that it represents a fluxoturbidite that interrupted the normal pelagic sedimentation in this part of the paleobasin.

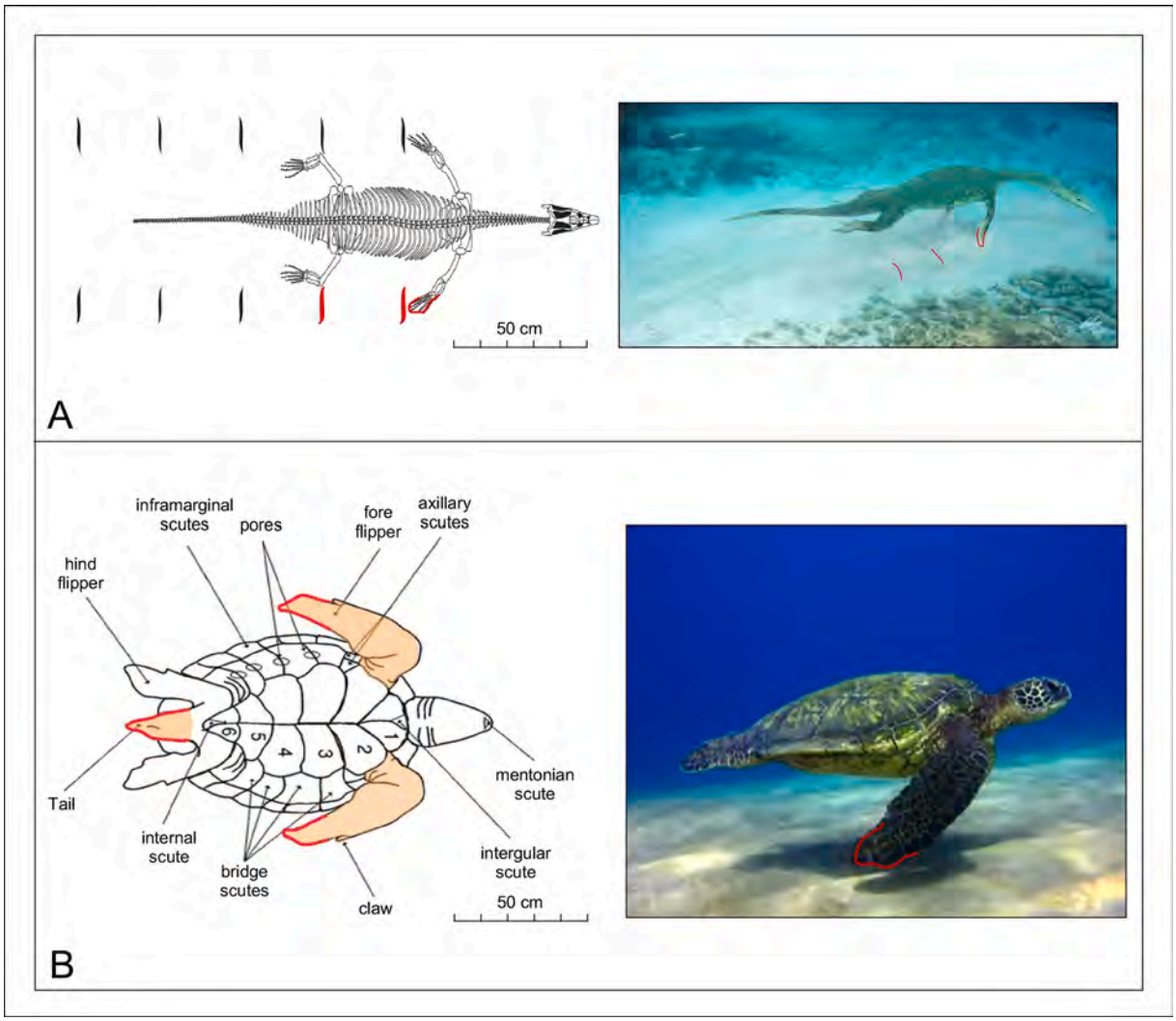

Fig. 5. A) Skeletal model of Triassic nothosaur *Lariosaurus*, viewed from above, paddling along and producing the tracks with its front paddles (highlighted in red), modified from Fig. 7a in Zhang et al. (2014). The artist scene picture on the right is borrowed from the original work of Brian Choo (modified from Fig. 8 in Zhang et al., 2014), which illustrates how a nothosaur makes progression tracks with its fore fins on a soft seafloor while stalking for a prey; B) Anatomic ventral view of a generic sea turtle with highlighted in color the body parts (i.e., the fore flippers and the tail) that would leave track marks on soft sediment while swimming or grazing underwater close to the seafloor. The scene picture on the right is a modified still frame from 0':55″ of a YouTube video showing a Hawaiian green sea turtle (*Chelonia mydas*) swimming close to the seafloor and brushing the soft sediment with the tip of its fore flipper (marked with a red contour line).
From https://www.youtube.com/watch?app=desktop&v=jsxvAzWmF9I.

Hawksbill turtles (*Eretmochelys imbricata*) that feed on sponges and other sessile invertebrates, permanently inhabit the same shallow water environment (e.g., Goatley et al., 2012, and references therein), which, in addition to supplying abundant food, provides shelter against open sea predators. The prevalence of sea turtle species in these environments leads us to hypothesize that the myriad trace fossils of the La Vela Slabs represent a mass displacement of a very large number of these animals (see dynamic box model in Fig. 6) that were lingering near the shallow water carbonate platform of Monte Cònero (see Fig. 7 for location), an ideal place for laying eggs but also a fertile ground for foraging. A sudden earthquake provoked a stampede toward the open sea in the opposite direction to the epicenter, or preceding a turbidity current that was triggered by the earthquake itself. Some of these panicking sea turtles swam close to the bathyal seafloor leaving footprints on the soft carbonate sediment, which were immediately covered and preserved under a calcilutitic fluxoturbidite triggered by the same earthquake (Fig. 6). Over the 200 m^2 area of the La Vela slab at Site 6, which we remotely mapped on a drone aerial orthophotograph (Fig. 2B), there may be as many as 1000 $\pm$ 300 of such footprints (i.e., a density of 5 $\pm$ 3 traces per square meter), and traces have been observed also on the slabs exposed on sites 5, 7, 8, 9, and 11, which represent the same pelagic layer.

These observations and assessments regarding the nature of the La Vela footprints need to be considered as an invitation to further specialistic studies on this amazing, perhaps unprecedented deep-water vertebrate ichnopaleontologic record. This field is foreign to the team of researchers co-authoring this contribution, which includes regional and environmental geologists, carbonate sedimentologists, stratigraphers, geophysicists, and micropaleontologists. On the other hand, we are taking advantage of this extraordinary discovery to frame such a dramatic event, i.e., a presumed *en masse* rush of marine reptiles (probably sea turtles), in the tectono-seismic, sedimentologic, and paleoenvironmental scenario of the Cretaceous Cònero Basin, in particular during the deposition of the Campanian Scaglia Rossa pelagic limestone. Following a review of the sedimentological and

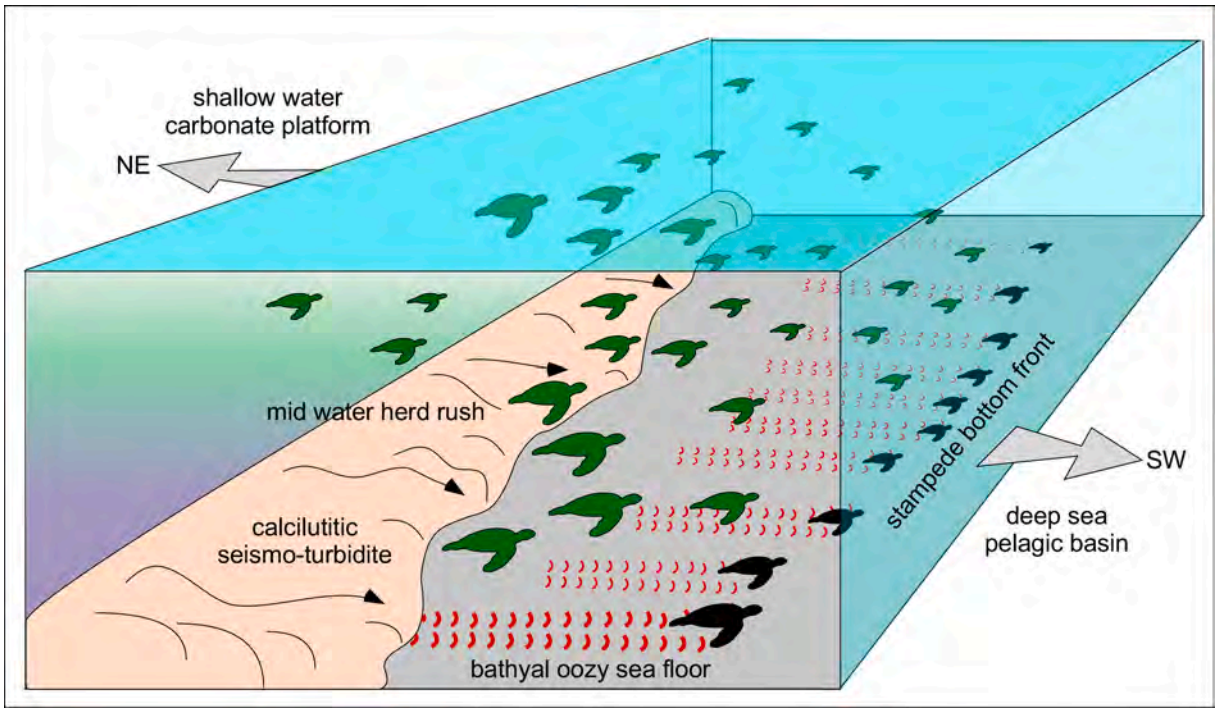

Fig. 6. Box model of a panicking sea turtle herd rushing toward the deep sea and away from the proximal environment of a shallow water carbonate platform from where a calciturbidite took off after being triggered by an earthquake. The red arched marks represent footprints left behind by a front of sea turtles swimming close to the oozy seafloor, which eventually were covered by the calcilutitic seismo-turbidite. This idealized scenario is related to the footprints found in the La Vela Beach Upper Section (BUS) at Monte Cònero, which is indicated in the paleogeographic map of Fig. 7B.

tectono-seismic history of the U-M Apennines, we will proceed with the description and documentation of our integrated stratigraphic analysis of the Campanian exposure along the La Vela Beach Upper Section (BUS), the location of which is indicated in Fig. 2A.

1.4. Geological background

The Scaglia Rossa Fm. of the Umbria and Marche regions of central Italy (Fig. 7A) is a thoroughly studied and well-dated sequence of rhythmically bedded pelagic limestones and marls (e.g., Alvarez, 2019 and references therein), locally interrupted by biocalcarenitic turbidites and soft sediment deformations (Montanari et al., 1989; Fig. 7B). It was deposited at the transition between rift-related subsidence, which started in the Late Triassic, and the beginning of convergent orogenic activity that led to the formation of the NE-progressing Northern Apennines accretionary wedge (e.g., D'Argenio, 1970; Alvarez et al., 1974; Channell et al., 1979; Castellarin et al., 1982; Treves, 1984; Marroni et al., 2001; Cornamusini et al., 2002; Argnani et al., 2006, and references therein). While major compression began in the Alps in the Early Cretaceous (Dewey et al., 1973), compression in the U-M basin did not begin until the Early Miocene.

Prior to the deposition of the Scaglia Rossa, the whole U-M basin was apparently flat and static, devoid of any manifestation of tectono-seismic activity such as synsedimentary faulting, slumping, and turbiditic sedimentation, as evidenced by the underlying Marne a Fucoidi and Scaglia Bianca formations that exhibit essentially uniform thicknesses everywhere throughout this region (Montanari et al., 1989; see Fig. 9). By contrast, the U-M Scaglia Rossa Fm. varies in thickness from 150 to 300 m regionally, indicating the creation of basinal topography through synsedimentary tectonic deformation (Alvarez and Lowrie, 1984; Chan et al., 1985; Alvarez et al., 1985; Montanari et al., 1989). As noted by Montanari (1988), the thicker sections of the Scaglia Rossa coincide with older syn-rift grabens (see also Fig. 1b in Bice et al., 2007), suggesting that the basinal topography was created by the reactivation of buried Jurassic normal faults. In summary, the Scaglia Rossa Fm. of the U-M region was a deep-water epeiric sea, perhaps as deep as 1500 m in the most distal areas of the paleobasin (Kuhnt, 1990), bordered to the south and east by shallow water carbonate platforms, and flanking aprons of detrital material, as shown in Fig. 7B. The limit of the platform-derived basinal deposits is relatively well known and is easily established by the distinctive shallow water fauna that compose the clasts of these grain flows, turbidites, and other mass flows.

In this general paleogeographic scenario, the Monte Cònero area was situated at the eastern edge of the U-M Basin. The Lower Cretaceous Maiolica Fm. is the oldest formation herein exposed (Fig. 8). Extensive exposures of this formation are located along the steep north-eastern flank of the Cònero anticline (Fig. 1 AB), particularly on the slopes above the aforementioned Due Sorelle (Fig. S2) and Grotta degli Schiavi beaches.

The upper part of the Maiolica Fm. is well exposed on both sides of the Due Sorelle promontory showing conspicuous soft sediment deformation (Fig. S2C and D). Slump folds have been observed in this upper part of the formation in other localities of Monte Cònero (e.g., Fig. S2E), all showing a north-eastern direction of sliding of unconsolidated, ductile carbonate sediment. The boundary between theMaiolica to the overlying Marne a Fucoidi Fm. is well exposed on the southern side of the Pirolo hill (Fig. 9A), and it is marked by the Selli Level, a radiolaritic black shale horizon representing the U-M expression of the Oceanic Anoxic Event 1a (OAE1a; e.g., Coccioni et al., 1987, 1989; Coccioni, 2020). A detailed lithostratigraphic model of the Pirolo succession is shown in Fig. 9A (from Coccioni et al., 1994), whereas a schematic model

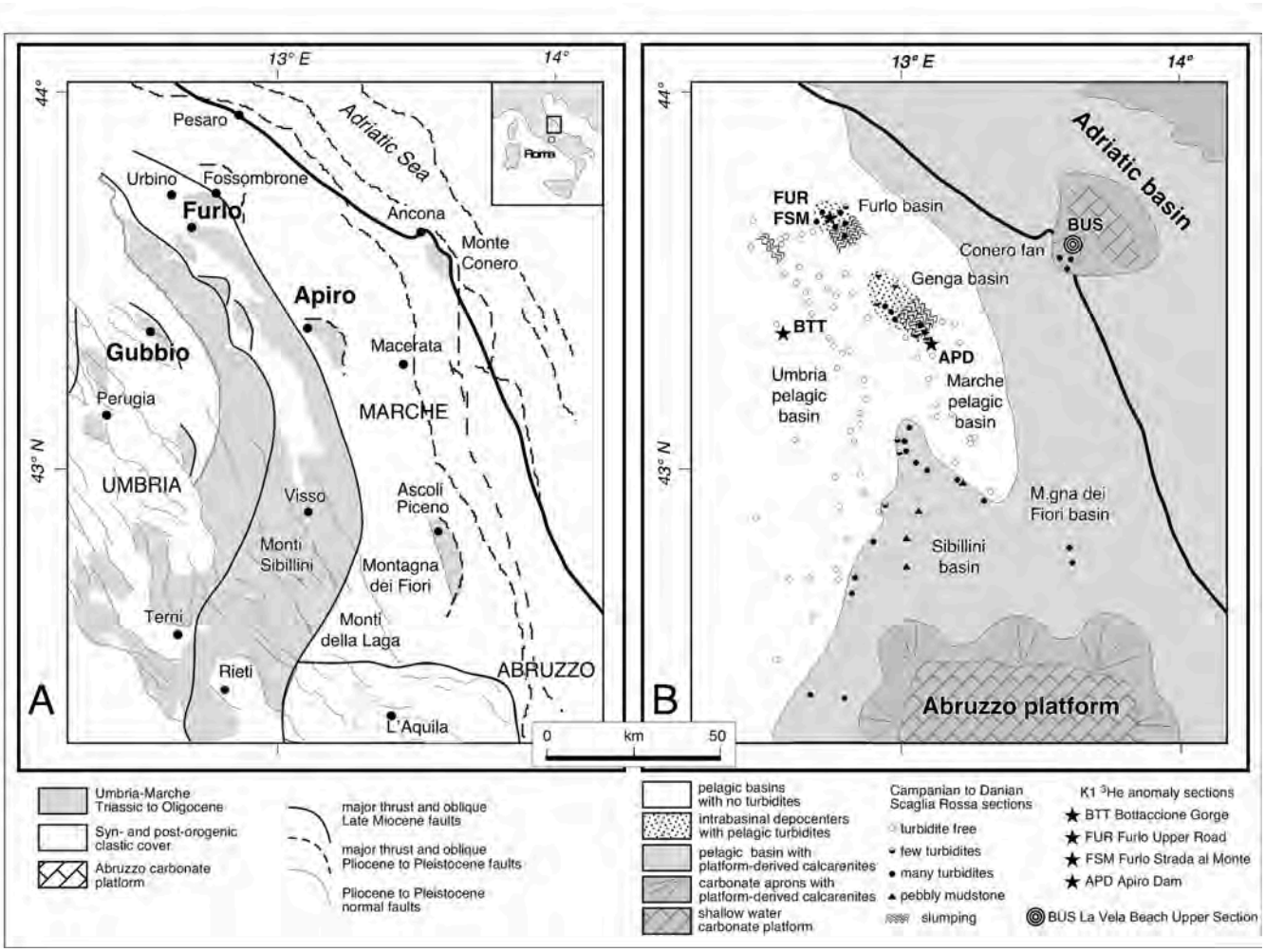

Fig. 7. A) Simplified geological map of the U-M Apennines; B) Palaeogeographic reconstruction of the U-M basin during the Late Cretaceous and early Paleocene. Latitudes and longitudes are relative to present day. The Adriatic coastline is indicated by a solid line. Filled and open circles and triangles represent exposed sections of the Scaglia Rossa Fm. The Furlo and Genga pelagic sub-basins, formed by reactivation of older normal faults, lie beyond the reach of material shed from the Adriatic and Abruzzo carbonate platforms, unlike Monte Cònero where the Campanian to Danian pelagic limestone is interbedded with calcarenites and calcirudites made up of bioclasts derived from a proximal carbonate platform (from Montanari et al., 2023).

of the Campanian megaslump that led to a conspicuous stratigraphic hiatus in the Cònero succession, is proposed in Fig. 9B to D. In summary, most of the Marne a Fucoidi, the whole Scaglia Bianca, and the lower part of the Scaglia Rossa formations are missing at Monte Cònero although pink and green-colored limestones and cherts of the Marne a Fucoidi can be found in landslide breccia deposits in a few localities such the aforementioned Davanzali quarry, the northern end of La Vela Beach, and on the bluffs at Il Clandestino and Le Terrazze beaches (Montanari et al., 2016). In recent years, as a consequence of ever stronger sea storms and consequent retreat of the coastline, a continuous ~25-m-thick section of Maiolica limestones was exposed along the La Vela Beach, here designated the La Vela Beach Lower Section (i.e., BLS; see synoptic Fig. 10A to F, and figure caption therein).

Past a landslide scree containing pinkish limestone breccia derived from the overlying Marne a Fucoidi Fm (Fig. 10 B), and overpassing a rocky notch, the stratified bedrock of the Cònero succession comes back to the surface, clean and well exposed along the supralittoral zone in a ~40-m-thick section, here named La Vela Beach Upper Section (BUS in Fig. 2A), where at meter level 30.7 we have identified the pelagic limestone bed with the footprints (see synoptic Fig. 11). The results of our integrated stratigraphic analysis of this La Vela Beach Upper Section will be described and documented in detail in the RESULTS chapter 3 of this paper.

2. Materials and methods

With the permission of the Cònero Park Authority, we first surveyed the La Vela area using a small drone (DJI Spark®), taking high-resolution digital photographs of Site 6 slab from a low elevation (~30 m) orthogonal to the exposed surface, as well as orthophoto aerial strips to construct a 3D point-cloud model of the slab. We then logged the stratigraphic sections exposed along the littoral of La Vela, including the Maiolica outcrop of the La Vela Beach Lower Section (BLS) and the Scaglia Rossa La Vela Beach Upper Section (BUS), using a foldable meter stick, marking the section with colored chalk at 1 m intervals, and finally photographing the outcrop in 2 or 3 m intervals. Hand samples of calcarenite and calcilutite were collected using a rock hammer whereas oriented, 23-mm-diameter, 40-mm-long core samples were collected at 2.5 m intervals from the BUS section using a cordless power drill with a dry concrete cup cutter for paleomagnetic analysis. Rock samples, washed residues, and thin

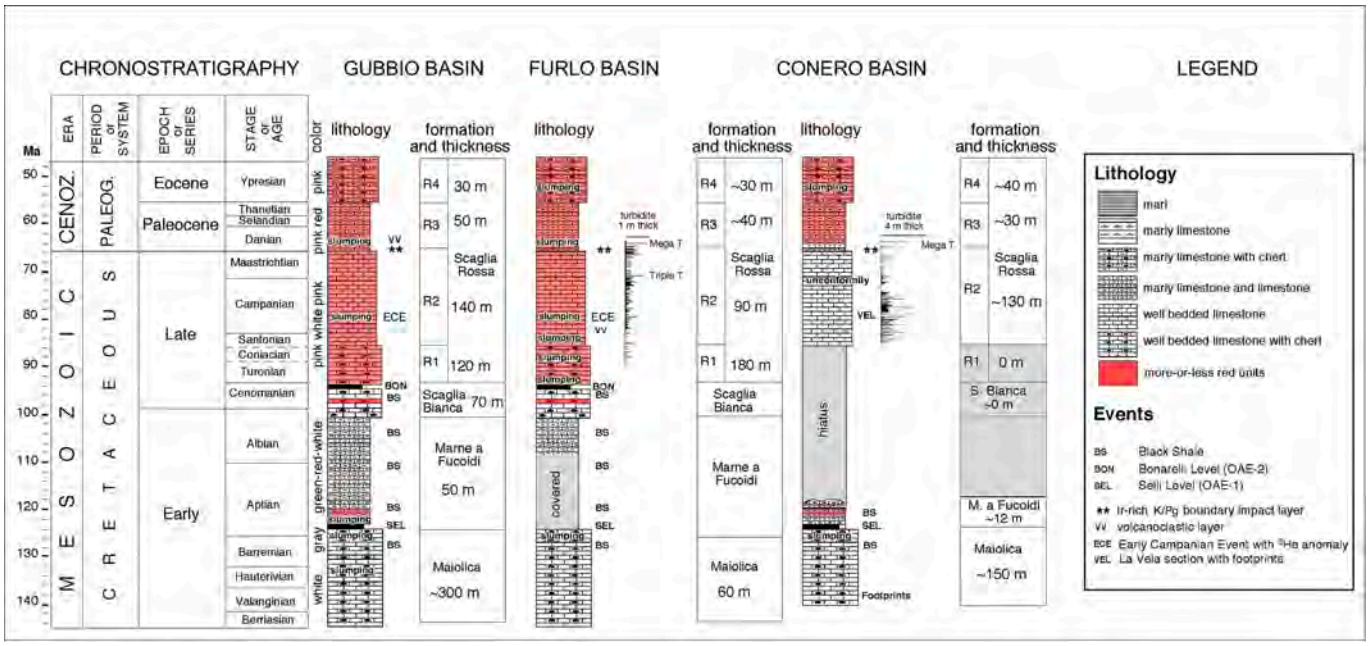

Fig. 8. Lower Cretaceous – Eocene integrated stratigraphy of the U-M sedimentary succession in the Gubbio, Furlo, and Cònero basins (see Fig. 7).

sections are deposited at the Osservatorio Geologico di Coldigioco (Italy), while magnetostratigraphic cores and offcuts are stored at the Department of Geosciences, NTNU (Norway).

2.1. Magnetostratigraphy

The alternating field (AF) demagnetization of magnetic remanence was measured using an Applied Physics Systems Model 755 cryogenic magnetometer at the Geological Survey of Norway. A noise floor for the magnetometer of ~5 × 10^{-10} Am^2 (~8 × 10^{-5} A/m for specimens of the size used in this study) is inferred by the observation that intensities below this approximate value recorded wildly varying magnetic directions. The characteristic paleomagnetic vector was calculated for those samples demonstrating a stable direction over consecutive steps using principal component analysis (Kirschvink, 1980) as implemented in PuffinPlot (Lurcock and Wilson, 2012). Demagnetization sequence and orthogonal vector diagrams for all samples and compiled principal component analysis results are presented in supplemental materials. Volume-normalized magnetic susceptibility was measured on an AGICO MFK1-A Kappabridge at the Norwegian University of Science and Technology. To quantify the magnetic mineral content and infer the mineral phase(s), magnetic hysteresis loops using fields up to 1.1 T and isothermal remanent magnetization sequences were acquired using a Princeton Measurements Corp. MicroMag 2800 vibrating sample magnetometer at ambient temperature. Raw data files of the magnetic measurements used in this study are available at https://doi.org/10.18710/S081GT.

2.2. Biostratigraphy

Standard thin sections were prepared for each collected hand and drill core sample at the Geological Observatory of Coldigioco for microfacies analysis using a Zeiss petrographic microscope. About 200 g of selected hand samples originally labelled as 2W (~2 m in the BUS section), 4B (~18 m in the BUS section), CON-VEL 5, 6, and 9.2 (equivalent to 30.7 m in the BUS section), and CON-VEL 9.1 (equivalent to 30.8 m in the BUS section), as well as samples at meter levels 32, 34, 36, 38, and 40 from the upper BUS section, were processed for planktonic foraminifera species classification and benthic foraminifera paleodepth assessments at the University of Urbino using the cold acetolysis washing technique. The same microfacies and micropaleontological analytical treatment was applied for samples 16.1, 16.2, 16.5, and 16.7 m from the BLS section. They were mechanically disaggregated into small fragments (3–8 mm) and treated following the cold acetolysis technique of Lirer (2000) by sieving through a 40 μm mesh and drying at 50 °C to avoid loss of the very small specimens that may be significant for paleoecological and biostratigraphic assessments. Some experiments were conducted with varying acid concentrations (20–80 %) and reaction times (3–12 h), until the methodology guaranteeing the best results was identified. This cold acetolysis method enables the extraction of generally easily identifiable foraminifera even from indurated limestones. It offers the possibility of accurate taxonomic determination and detailed analyses of planktonic foraminiferal assemblages, thus providing the precise placement of several primary and secondary biohorizons and zonal boundaries and recognition of previously undetected bioevents (e.g., Coccioni, 2020; Coccioni et al., 2022).

Planktonic and benthic foraminifera from the washed residues were studied under a stereomicroscope. Observations were conducted on size fractions separately: 40–75 μm; 75–100 μm; 100–125 μm; 125–150 μm; 150–180 μm; 180–250 μm; and >250 μm. The total abundance of planktonic foraminifera based on entire >40 μm fraction was annotated as follows: absent; very rare; rare; few. Preservation was assigned as follows: poor; moderate; and good. Taxonomic concepts for genera and species identification followed the online Mikrotax database (http://mikrotax.org/pforams/index.php?dir=pf_mesozoic) where the type material for most species is illustrated by new scanning electron microscopy (SEM) images (Huber et al., 2016). The planktonic foraminiferal standard zonation of Coccioni and Premoli Silva (2015) was applied. With regards to the assessment of the paleodepth from the benthic foraminiferal associations, the bathymetric subdivision of van Morkhoven et al. (1986) and Berggren and Miller (1989), was followed (i.e., inner neritic [0

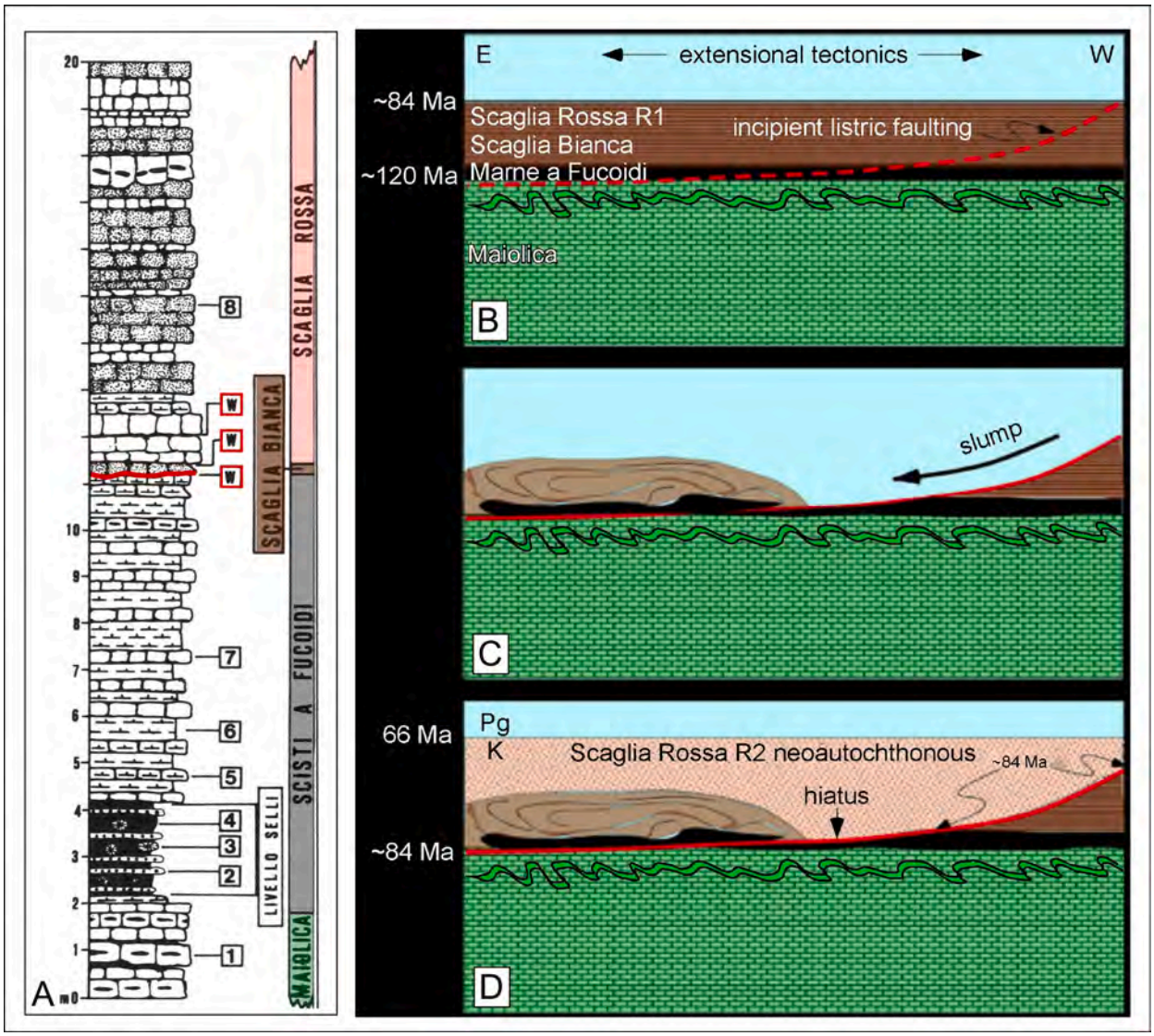

Fig. 9. A) Detailed stratigraphy of the Cretaceous sedimentary succession at the Pirolo hill of Monte Cònero resulting from the mega slump triggered by a major seismo-tectonic event in the Late Cretaceous (from Coccioni et al., 1994). The red frames with "W" indicate 3 stratigraphic gaps suggested by planktonic foraminiferal assemblages determined by one of us (R.C.) in samples probably collected from the same layers indicated by the letters **a** and **b** in Fig. S3F. The red line in the stratigraphic log represents a paraconformity coinciding with the detachment surface of the megaslump represented in the block diagrams B, C, and D. 1 = limestone with chert; 2 = Radiolarite; 3 = Pyrite nodules; 4 = Black shale; 5 = Marly limestone; 6 = Marl; 7 = Calcilutitic limestone; 8 = Biocalcarenitic limestone. Note that Scisti a Fucoidi is synonym of Marne a Fucoidi; B to D is a schematic model of the Upper Cretaceous mega slump at Monte Cònero as derived from the stratigraphy of the Pirolo hill section; B) Incipient listric normal faulting during an extensional seismo-tectonic regime; C) Slumping triggered by a major earthquake; D) Sedimentation of the neoautochthonous Scaglia Rossa R2 pelagic limestone with resulting hiatus at the base. The undulating lines in the upper part of the Maiolica Fm. represent a widespread horizon containing soft sediment deformations.

30 m], middle neritic [30–100 m], outer neritic [100–200 m], upper bathyal [200–600 m], middle bathyal [600–1000 m], lower bathyal [1000–2000 m], upper abyssal [2000–3000 m] and lower abyssal [>3000 m]).

3. Results: integrated stratigraphy of the La Vela sections

The Lower Cretaceous pelagic limestones of the Maiolica Fm., steeply dipping toward the NE, and the overlying Campanian pelagic limestones interbedded with calcarenitic and calcilutitic turbidites of the Scaglia Rossa Fm. are exposed along a ~200-m-stretch of the supralittoral splash zone around the La Vela sea stack (Fig. 2A). The lithostratigraphy of the Maiolica BLS section is synoptically described in Fig. 10A, whereas the integrated litho- and magneto-stratigraphy of the Scaglia Rossa section (BUS) is illustrated in Fig. 11.

3.1. Lithostratigraphy of the Maiolica BLS section

Of the 25-m-thick BLS section not much can be said other than that the Maiolica exhibits here its most typical lithofacies characterized by thin-to-medium thick, white to gray, micritic limestone beds often containing chert nodules, sometimes interbedded with dark gray bituminous marls or actual black shales, and also gray to black continuous chert beds (see Fig. 10B to F). Acetolysis-washed residues of limestone samples taken at 16.1, 16.2, 16.5, and 16.7 m were dominated by radiolarian skeletons and very rare tests of benthic foraminifera, most of which were partially dissolved and not identifiable. In the absence of biostratigraphic evidence for the age for this short Maiolica section, it is not possible to correlate it with the ~200-or-more-m-thick Maiolica exposed on the cliffs and crags around the Due Sorelle promontory (see Fig. S2A). However, the presence of soft-sediment slump folds at

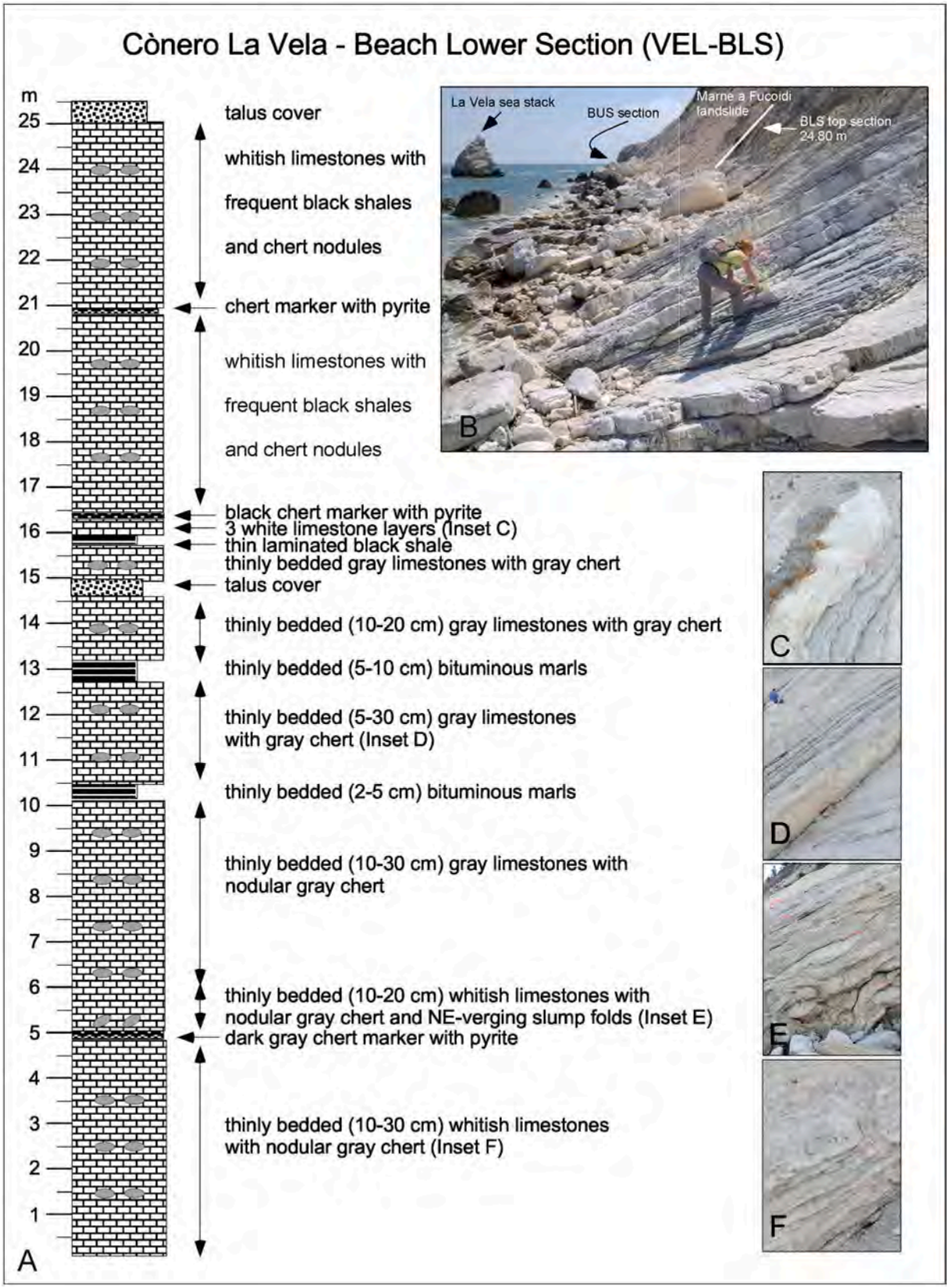

Fig. 10. Synoptic lithostratigraphy of La Vela Beach Lower Section (BLS) belonging to the Maiolica Formation. A) Schematic lithostratigraphy of the BLS section with field annotations; B) Panoramic view of the upper part of the section; C, D, E, and F, close-up photographs of portions of the section annotated in A.

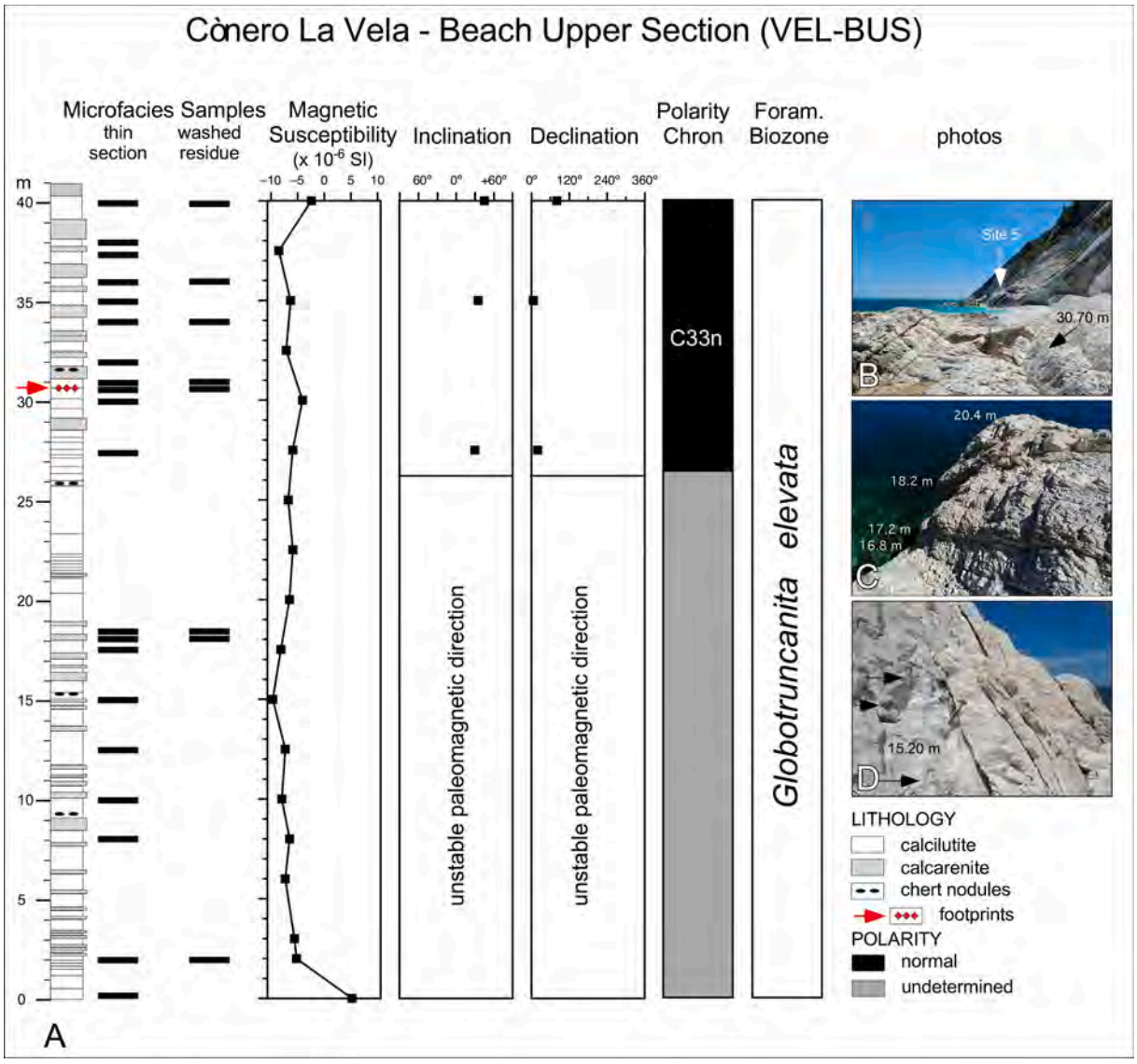

Fig. 11. Synoptic stratigraphic model of the La Vela Beach Upper Section (BUS) belonging to the Scaglia Rossa Fm. The recognized footprints fall at meter level 30.7. The whole section pertains to the lowermost Campanian *Globotruncanita elevata* planktonic foraminiferal zone. Volume-normalized susceptibility graph indicates position of all collected paleomagnetic samples. Paleomagnetic inclination and declination in bedding-corrected coordinates.

5.5 m in the BLS section (Fig. S2E) may suggest that the upper part of this formation on either side of the Due Sorelle promontory is characterized by pervasive soft sediment deformation (see Fig. S2C–D).

3.2. Integrated stratigraphy of the Scaglia Rossa BUS section

3.2.1. Lithostratigraphy

The lithostratigraphy of the 40-m-thick BUS section is characterized by an alternation of fine calcarenitic turbidites and white, homogeneous calcilutitic limestones, the ultrafine texture of which is not visible in hand sample even with the aid of a hand lens, but requires examination in thin section using a petrographic microscope (Fig. 11A). Figure 12 summarizes the different microfacies of these calcarenitic and calcilutitic limestones. One aspect to be noted is that some of these calcilutites are evidently pelagic, i.e., characterized by planktonic foraminiferal tests suspended in a micritic matrix (see Fig. 12A, B, and D; see also Fig. 4E), while other calcilutites are clearly detrital (Fig. 12C, E, F, and G; see also Fig. 4G). Moreover, unlike the Maastrichtian and lowermost Danian calcarenites and calcirudites of the Monte Còmero succession including the Marchesini (or MegaT) marker bed, which are made up of carbonate clasts derived from a proximal shallow-water carbonate platform, including benthic macroforaminifera (i.e., orbitoids), rudists, bryozoans, corals, etc (Montanari, 1979; Coccioni et al., 1994), the fine calcarenites and turbiditic calcilutites of the Campanian succession at La Vela are composed of reworked pelagic material, such as planktonic foraminifera, inoceramid prisms, calcispheres, etc.

3.2.2. Planktonic foraminifera assemblage and biozone assessment

Planktonic foraminifera occur in all acetolysis-washed residues and all but 3 thin sections (see Table S1.). However, their preservation and abundance vary widely from sample to sample, ranging from very poor to good and from very rare to common, respectively. Species diversity parallels the observed fluctuations in abundance. The most abundant and diversified samples studied in cold acetolysis washed residues were CON-VEL 2W (~2 m level in

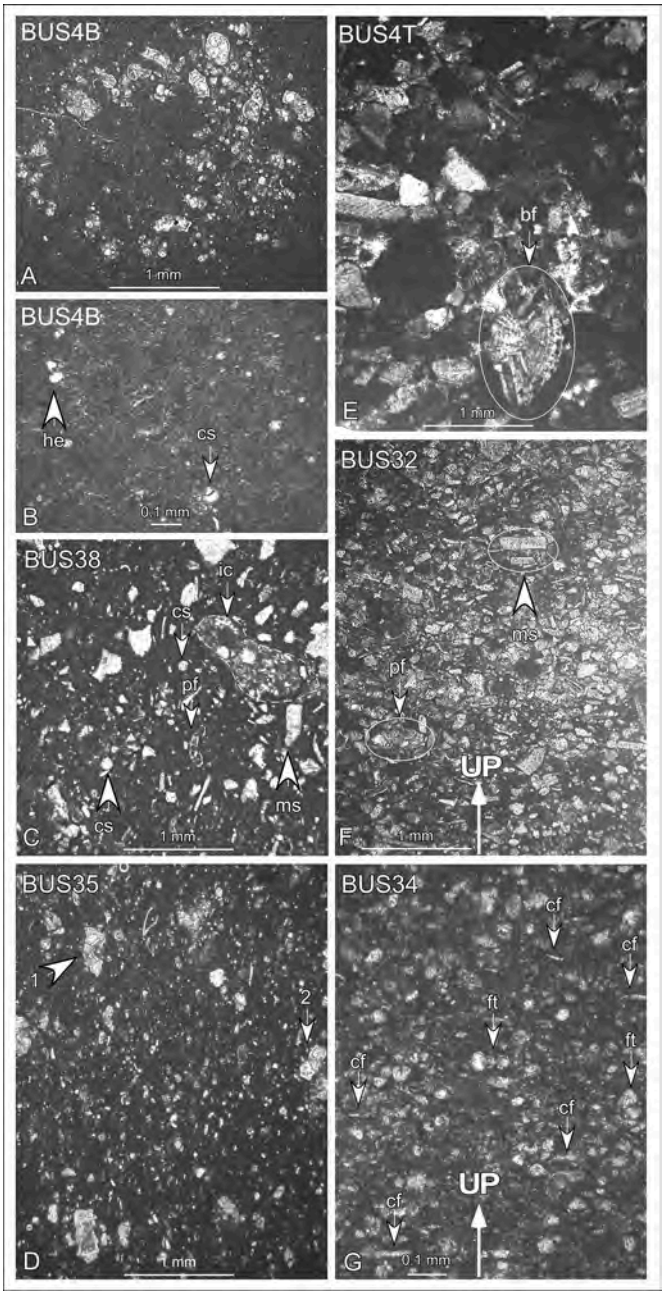

Fig. 12. Black-and-white microphotographs of microfacies as seen in thin-section from the Campanian Scaglia Rossa Fm. exposed at the La Vela Beach Upper Section. A) Bioturbation trace filled with planktonic foraminiferal debris in an otherwise white, homogeneous calcilutite at Site 4 from ~18 m above the base of the BUS section shown in Fig. 11A. B) The matrix of the same BUS 4B sample can be described as a wackestone, which includes heterohelicid tests (→he), and calcispheres (→cs); C) A calcarenite from Site 4 at ~18 m above the base of the BUS section exhibiting a polygenic detrital composition including: muddy wackestone intraclasts (→ic), planktonic foraminifera (e.g. →pf = *Marginotruncana pseudolinneiana*), calcispheres (→cs), and mollusk shell fragments (→ms); D) Pelagic mudstone from meter level 35 in the BUS section shown in Fig. 11A, containing well-preserved planktonic foraminiferal tests (e.g., →1 = *Globotruncanita elevata*, and →2 = *Globotruncana linneiana*); E) Calcarenite at Site 4–18 m above the base of the BUS section comprising rotaliids foraminiferal tests (→bf) along with fragments of various carbonate shallow water organisms such as bryozoans, mollusk shells, benthic forams, echinoderms, corals, and calcareous algae; F) Calcarenitic turbidite at meter level 32 in the BUS section shown in Fig. 11A (way up indicated by a white arrow), mostly made up of prismatic fragments of mollusk shells (possibly inoceramids), and rare planktonic foraminiferal tests (e.g. →pf = *Marginotruncana schneegansi*); G) Grain-supported calcilutitic turbidite at meter level 34 in the BUS section shown in Fig. 11A (way up indicated by a white arrow), made up of fragments of small foraminiferal tests (→ft) and plane-parallel-aligned calcite filaments (→cf).

the BUS section with 215 identified specimens), and CON-VEL 5 (equivalent to 30.7 m in the BUS section with 300 identified specimens; see Table S1). Some 30 specimens were recognized and identified in a thin section of sample CON-VEL 9.1 (equivalent to 30.8 m in the BUS section) and a few others in thin section of sample CON-VEL 4B (~18 m in the BUS section), as well as in a thin section of sample CON-VEL 9.2 (equivalent to 30.7 m in the BUS section; see Table S1).

According to the ranges of Late Cretaceous planktonic foraminifera species provided by Miniati et al. (2020) from the Campanian GSSP in the Bottaccione Gorge near Gubbio (Gale et al., 2023), the occasional occurrence of *M. schneegansi* (Table S1) is probably due to reworking. On the basis of the occurrence of *Globotruncanita elevata* along with marginotruncanids, and the absence of *Dicarinella asymetrica* and *Contusotruncana plummerae*, the BUS section lies in the lower Campanian *Globotruncanita elevata* Zone.

3.2.3. Benthic foraminifera identification and paleodepth estimate

Benthic foraminifera occurred in a few samples and their abundance is commonly very low. Similar to planktonic foraminiferal specimens, the preservation varied from very poor to good. The P/B ratio in all analyzed samples is invariably >99 %, which is consistent with deposition at bathyal or greater depths (e.g., Gibson, 1989; van der. Zwaan et al., 1990). Benthic foraminiferal assemblages are mostly represented by calcareous genera including *Nuttallides*, *Anomalinoides*, *Stensioeina*, *Osangularia*, *Gavelinella*, and *Oridorsalis*. The most common agglutinated foraminiferal genus is *Gaudryina*. On the basis of the paleobathymetric distribution of these genera as documented by Sliter and Baker (1972) and Nyong and Olsson (1984), a bathyal deposition can be inferred.

A more precise inference has been derived from paleobathymetric models and interpretation as well as upper depth limits of Sliter and Baker (1972), Berggren and Aubert (1975), Tjalsma and Lohmann (1983), Olsson and Nyong (1984), Nyong and Olsson (1984), van Morkhoven et al. (1986), Widmark (1997), Widmark and Speijer (1997), Alegret and Thomas (2001), Cetean et al. (2011) and Frontalini et al. (2016). The most abundant calcareous foraminiferal species are *Anomalinoides nobilis* (Brotzen 1948), *Stensioeina pommerana* (Brotzen 1936), *Osangularia cordieriana* (d'Orbigny, 1840), *Nuttallides truempyi* (Nuttall, 1930), *Gavelinella beccariiformis* (White, 1928), *Gyroidinoides nitidus* (Reuss, 1844) and, among the agglutinated, *Gaudryina pyramidata* (Cushman, 1926). Most of these occur at a middle bathyal depth such as *A. nobilis* (Cetean et al., 2011), *S. pommerana* (Widmark, 1997), *O. cordieriana* (Sliter and Baker, 1972; Olsson and Nyong, 1984), *N. truempyi* (van Morkhoven et al., 1986), *G. beccariiformis* (van Morkhoven et al., 1986; Widmark and Speijer, 1997), and *G. nitidus* (Sliter and Baker, 1972), whereas *G. pyramidata* at an upper bathyal (van Morkhoven et al., 1986; Widmark and Speijer, 1997). On the basis of these observations and considering the upper depth limits of the identified benthic foraminiferal taxa, a middle-to-lower bathyal depositional environment can be inferred for the lower Campanian Scaglia Rossa basin of Monte Cònero.

3.2.4. Magnetic carriers and magnetostratigraphy

The limestones of the BUS section are without exception very weakly magnetic: only one specimen exhibits positive magnetic susceptibility, and the average of the remaining samples is -6.5×10^{-6} SI (Fig. 11A). The dominance of the diamagnetic signal that generates these negative values indicates a very low content of ferromagnetic (*s.l.*) material. Of the 12 samples from which hysteresis loops were measured, 9 exhibited a response that was not purely diamagnetic. The saturation magnetization (M_s) of these 9 samples ranged from 1.1 to 6.7 $\times$ 10^{-5} Am^2/kg (Table S2). Mitchell

et al. (2021) reported that biogenic magnetite is the dominant magnetic carrier in the Scaglia Rossa, which would indicate that the magnetite content of these samples ranges from 0.000012 to 0.000073 %. Channell et al. (1982) observed the presence of goethite and hematite in samples from other Scaglia Rossa localities, and because their saturation magnetization is ~200 times weaker than that of magnetite (Dunlop & Özdemir, 1997), such phases could be present in concentrations 2 orders of magnitude larger than those calculated for magnetite.

The presence of coexisting high-coercivity magnetic phases such as hematite and goethite can be tested using isothermal remanent magnetization (IRM) experiments, which measure the coercivity distribution of the sample (Fig. S3). The IRM of all samples is dominated by magnetite, with more than 60 % and in many specimens, fully 100 % of IRM controlled by carriers with coercivities of remanence <300 mT, typical of magnetite. Specimens from BUS24–22.5, BUS24–27.5, and BUS24–37.5 clearly show the presence of an additional phase with a coercivity >300 mT, as indicated by the smaller increase in magnetization acquired above fields of this value (Figs. S3G, S3H, S3K). BUS24–15.0 and BUS24–35.0 also show a steady increase in IRM up to the maximum field of 1.1 T, which may also indicate a high-coercivity phase, but there is also a high level of noise in these data, so it is difficult to confidently identify trends. Both goethite and hematite exhibit coercivities much greater than that of magnetite (Rochette et al., 2005) and thus are potential sources for this high-coercivity component and in the absence of pink coloration in these samples, goethite seems a likely candidate for this signal. Due to limited access to the cryogenic magnetometer that these samples demand, we were unable to carry out thermal demagnetization or the

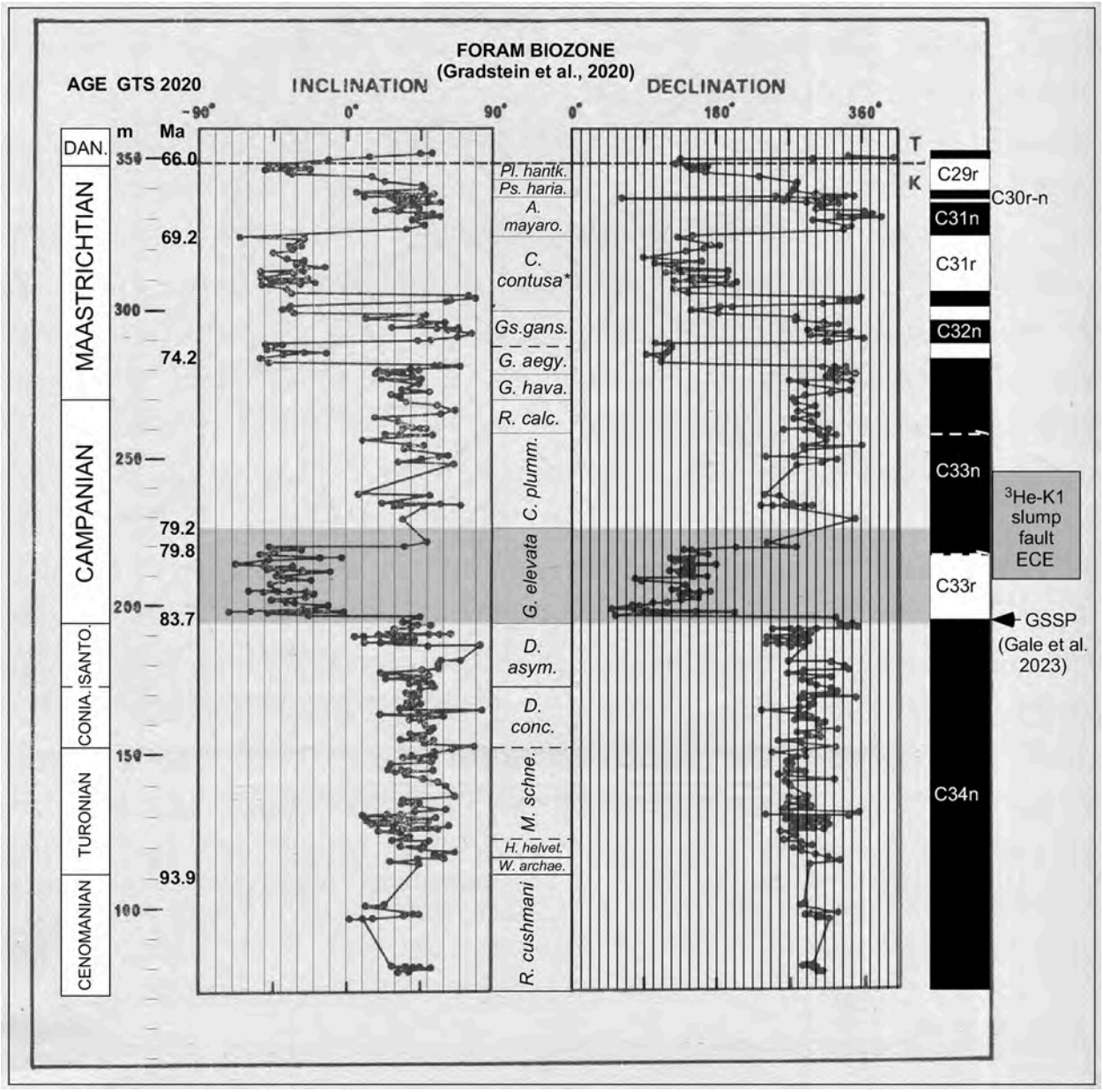

Fig. 13. Original paleomagnetic record of the Bottaccione section (Gubbio) from Fig. 2 in Lowrie and Alvarez (1976) with an updated foraminiferal biostratigraphy and chronostratigraphy (from Gradstein et al., 2020) and with proper adjustments from Coccioni and Premoli Silva (2015). The *Globotruncanita elevata* Zone, to which the La Vela Beach section (BUS) is here attributed, is highlighted with a gray band.

Lowrie test (Lowrie, 1990) that would unambiguously identify these additional phases and evaluate their role in paleomagnetic recording.

The low magnetic mineral content of samples from this locality resulted in remanence intensities (average of untreated samples: 2.0×10^{-4} A/m, Table S3) that commonly fell below the estimated noise floor of the cryogenic magnetometer. Furthermore, due to an instrument fault the demagnetization sequences for samples from the lowest 15 m were incomplete and are insufficient data points to calculate a characteristic paleomagnetic vector. The demagnetization sequence for most samples was noisy and did not decay linearly to the origin (Fig. S4), except for those from meter levels 35, 40, and to a lesser extent, 27.5 (BUS24–35.0, BUS24–40.0, and BUS24–27.5). The mean destructive field of these well-behaved samples is 14–27 mT and their remanence intensity is reduced by 90 % by fields up to 80 mT, values which are consistent with magnetite as the magnetic carrier. The demagnetization sequence from BUS24–35.0 and BUS24–40.0 showed a possible second component in the first steps (up to 10 and 5 mT, respectively), which may represent a viscous overprint and was therefore excluded from the characteristic remanence vector calculation.

In addition to these magnetite-bearing samples, those from meter levels 17.5, 22.5, and 37.5 (BUS24–17.5, BUS24–22.5, BUS24–37.5) also yielded magnetic vectors that were stable under AF demagnetization, although they were not properly cleaned by the technique. The orthogonal vector diagrams of these samples (Fig. S4) show that the vector does not decay to the origin, largely reflecting that the remanence intensity does not decrease monotonically with increasing AF steps. The stereonet plots of the demagnetization sequence, however, indicate that the direction is stable. IRM analyses (Fig. S3) of BUS24–22.5 and BUS24–37.5 clearly show the presence of a high-coercivity phase; it is likely that the magnetic carrier in these samples does not respond to moderate alternating fields and would require thermal demagnetization to correctly measure the paleomagnetic vector. We note that the polarity of these three samples is normal, although because they have not been demagnetized, this interpretation cannot be considered a tenable paleomagnetic vector and is not included in the magnetostratigraphy of this section.

The characteristic vectors that could be measured from the three magnetite-dominated specimens from the section are all of normal polarity (Fig. 11A). There is a high degree of scatter $\alpha 95 = 51^\circ$ (Fisher, 1953), and an average declination of 31.3° and inclination of 41.2°. The inclination values are not dissimilar to those reported from normally-magnetized Scaglia Rossa samples (e.g., 44°: Lowrie and Alvarez, 1976, 1977; see Fig. 13), but the declination strongly deviate from the literature value of 312°. The scatter in this data set potentially reflects both the weak remanence and limited number of samples; additional paleo- and rock magnetic studies would be needed to test if the deviations observed here are consistent and to identify their cause. Nevertheless, the combination of the biostratigraphy with the normal polarity inferred from the paleomagnetic inclination indicates that the upper part of the BUS section records magnetochron C33n. This interpretation is consistent with reported identification of magnetochron C33r in a Scaglia Rossa section lower in the Monte Cònero stratigraphy. Chan et al. (1985), while collecting samples for paleomagnetic analysis in sections of the Scaglia Rossa Fm. throughout the U-M Apennines, obtained a few specimens from the base of the formation at the Due Sorelle Beach, i.e. the same outcrop described by Montanari (1979) shown herein as Fig. S2G. Those samples yielded a reverse magnetic polarity and Campanian planktonic foraminifera identified in thin section, which suggested a lowermost Campanian C33r chron. The paleomagnetic data from this section were judged unimportant for the scope of the final paper and hence were not published (Lung Chan, personal communication, November 2024), but the identification of an early Campanian age was confirmed by Coccioni et al. (1994).

4. Summary and conclusions

The Lower Cretaceous-to-Pliocene stratigraphic succession of Monte Cònero, on the easternmost margin of the Umbria-Marche paleo-basin (northeastern Apennine fold-and-thrust belt of central Italy), contains a ~30-Myr-long hiatus derived from a seismically-induced mega slump that occurred in the Campanian. Extensional seismo-tectonic activity in the U-M basin actually started in the Turonian after a ~25-Myr-long period (i.e., mid Aptian to mid Turonian) of tectonic quiescence, and continued up to the Eocene with evident manifestations of seafloor instability, such as soft-sediment slumping and frequent turbiditic events, in many parts of the paleo-basin, including Monte Cònero. In short, calcilutitic and calcarenitic turbidites interbedded with planktonic foraminifera-bearing pelagites of the Campanian Scaglia Rossa Fm. represent the neo-autochthon sediment capping the detachment scar plane of the Monte Cònero mega slump.

On a secluded northeastern limb of the Monte Cònero anticline, which steeply dips to the Adriatic Sea, a group of free climbers by chance discovered myriad footprint traces deeply impressed on a vast exposed top surface of one of the Scaglia Rossa pelagic limestones. The footprints probably represent a stampede of panicking sea turtles that were mobilized *en masse* by an earthquake. These tracks were covered by a fluxoturbidite triggered by the same earthquake. The same layer is exposed in a 40-m-thick section along the littoral zone below, here designated La Vela Beach Upper Section (BUS in Figs. 2A and 11A). This section provides the ability, through biostratigraphic analysis, to place the footprint layer in the lower Campanian *Globotruncanita elevata* Zone during a period of normal magnetic polarity, likely the lowermost part of magnetochron C33n (see Fig. 13).

This calamitous earthquake coincides temporally with the so-called Early Campanian event (ECE; Sabatino et al., 2018), which represents a sudden climate change that, as documented by Montanari et al. (2023, and references therein), was caused by an extraterrestrial event such as an asteroidal breakup. This was followed by a cascade on Earth of comminuted asteroidal material including ^{3}He-rich interplanetary dust particles, which altered the transparency of the atmosphere and led to global climatic cooling. As described by Bice et al. (2007), the small eustatic sea level fluctuation caused by this climate change modified the rheology of the U-M paleobasin's crust, which was under tension during a phase of re-exhumed extensional tectonism, causing an increase of seismic activity that triggered soft sediment slumping and seismo-turbidites. Our litho-, bio-, and magneto-stratigraphic study of a new, 40-m-thick section of Campanian Scaglia Rossa at Monte Cònero, which includes a layer with reptile footprints at meter level 30.7, records this unstable seismo-tectonic period.

CRediT authorship contribution statement

Paolo Sandroni: Writing – review & editing, Investigation, Conceptualization. **Nathan S. Church:** Writing – review & editing, Visualization, Investigation, Formal analysis, Data curation. **Rodolfo Coccioni:** Writing – review & editing, Investigation, Formal analysis, Conceptualization. **Fabrizio Frontalini:** Writing – review & editing, Investigation, Formal analysis, Conceptualization. **Maurizio Mainiero:** Writing – review & editing, Investigation. **Alessandro Montanari:** Writing – review & editing, Writing – original draft, Visualization, Resources, Project administration, Investigation, Formal analysis, Conceptualization.

Declaration of competing interest

The authors declare that they have no known competing financial interests or personal relationships that could have appeared to influence the work reported in this paper.

Acknowledgements

This research was financially supported by the non-profit association “Le Montagne di San Francesco” (www.coldigioco.org). We would like to thank the authorities of the Cònero Regional Park, i.e., President dott. Luigi Conte and Director dott. Marco Zannini, for the permission granted to us to study and sample the La Vela area on the secluded northeastern side of Monte Cònero. A special thank goes to free climbers Cristina Domogrossi, Andrea Gagliardini, and Stefano Recanatini for assisting us on the surveying of the La Vela Slabs. This manuscript was greatly improved by the recommendations of two anonymous reviewers and the guidance of editor Prof. Maria Rose Petrizzo. Finally, we would like to thank Martin Klug (Geological Survey of Norway) and Karl Fabian (Norwegian University of Science and Technology) for their assistance with the cryogenic magnetometer measurements.

Data availability

Data will be made available on request.

References

Alegret, L., Thomas, E., 2001. Upper Cretaceous and lower Paleogene benthic foraminifera from northeastern Mexico. Micropaleontology 47, 269–316. https://doi.org/10.2113/47.4.269.

Alvarez, W., 2019. A review of the Earth history record in the Cretaceous, Paleogene, and Neogene pelagic carbonates of the Umbria-Marche Apennines (Italy): Twenty years of the Geological Observatory of Coldigioco. In: Koeberl, C., Bice, D.M. (Eds.), 250 Million Years of Earth History in Central Italy: Celebrating 25 Years of the Geological Observatory of Coldigioco, vol. 542. Geological Society of America Special Paper, pp. 1–58. https://doi.org/10.1130/2019.2542(01).

Alvarez, W., Cocozza, T., Wezel, F.C., 1974. Fragmentation of the Alpine orogenic belt by microplate dispersal. Nature 248, 309–314. https://doi.org/10.1038/248309a0.

Alvarez, W., Lowrie, W., 1984. Magnetic stratigraphy applied to synsedimentary slumps, turbidites, and basin analysis: The Scaglia limestone at Furlo (Italy). Geological Society of America Bulletin 95, 324–336. https://doi.org/10.1130/0016-7606(1984)95<324:MSATSS>2.0.CO;2.

Alvarez, W., Colacicchi, R., Montanari, A., 1985. Synsedimentary slides and bedding formation in Apennine pelagic limestones. Journal of Sedimentary Petrology 55, 720–734. https://doi.org/10.1306/212F87CE-2B24-11D7-8648000102C1865D.

Angeli, M.C., 1999. La Falesia tra Ancona e Sirolo. Consiglio Nazionale delle Ricerche (CNR). Istituto per la Protezione Idrogeologica (IRPI), Regione Marche Servizio Protezione Civile, Decreto di Giunta Regionale (DGR) 02/96 (3633), 1–45.

Argnani, A., Fontana, D., Stefani, C., Zuffa, G.G., 2006. Palaeogeography of the Upper Cretaceous–Eocene carbonate turbidites of the Northern Apennines from provenance studies. In: Moratti, G., Chalouan, A. (Eds.), Tectonics of the Western Mediterranean and North Africa, vol. 262. Geological Society, London, Special Publication, pp. 259–275. https://doi.org/10.1144/GSL.SP.2006.262.01.16.

Aringoli, D., Gentili, B., Materazzi, M., Pambianchi, G., Farabollini, P., 2014. Il ruolo della gravità nell'evoluzione geomorfologica di un'area di falesia: Il caso del Monte Conero (Mare Adriatico, Italia centrale). Studi Costieri 22, 19–32.

Arthur, M.A., Fischer, A., 1977. Upper Cretaceous–Paleocene magnetic stratigraphy at Gubbio, Italy. I. Lithostratigraphy and sedimentology. Geological Society of America Bulletin 88, 367–371. https://doi.org/10.1130/0016-7606(1977)88<367:UCMSAG>2.0.CO;2.

Baucon, A., Ferretti, A., Fioroni, C., Pandolfi, L., Serpagli, E., et al., 2023. The earliest evidence of deep-sea vertebrates. Proceedings of the National Academy of Sciences 1–137. https://doi.org/10.1073/pnas.2306164120, 120/137 e2306164120.

Berggren, W.A., Aubert, J., 1975. Paleocene benthonic foraminiferal biostratigraphy, paleobiogeography and paleoecology of Atlantic-Tethyan regions. Midway-type fauna. Palaeogeography, Paleoclimatology, Palaeoecology 18, 73–192.

Berggren, W.A., Miller, K.G., 1989. Cenozoic bathyal and abyssal calcareous benthic foraminiferal zonation. Micropaleontology 35, 308–320. https://doi.org/10.2307/1485674.

Bice, D., Montanari, A., Rusciadelli, G., 2007. Earthquake-induced turbidites triggered by seal level oscillations in the Upper Cretaceous and Paleocene of Italy. Terra Nova 19, 387–392. https://doi.org/10.1111/j.1365-3121.2007.00752.x.

Castellarin, A., Colacicchi, R., Praturlon, A., Cantelli, C., 1982. The Jurassic–Lower Pliocene history of the Anzio-Ancona Line (central Italy). Memorie della Societa Geologica Italiana 24, 325–336.

Cetean, G.C., Bălc, R., Kaminski, M., Filipescu, S., 2011. Integrated biostratigraphy and palaeoenvironments of an upper Santonian – upper Campanian succession from the southern part of the Eastern Carpathians, Romania. Cretaceous Research 32, 575–590. https://doi.org/10.1016/j.cretres.2010.11.001.

Chan, L.S., Montanari, A., Alvarez, W., 1985. Magnetic stratigraphy of the Scaglia Rossa: implications for syndepositional tectonics of the Umbria-Marches basin, Italy. Rivista Italiana di Paleontologia e Stratigrafia 91, 219–258.

Channell, J.E.T., D'Argenio, B., Horvath, F., 1979. Adria, the African promontory in Mesozoic Mediterranean palaeogeography. Earth-Science Reviews 15, 213–292. https://doi.org/10.1016/0012-8252(79)90083-7.

Channell, J.E.T., Freeman, R., Heller, F., Lowrie, W., 1982. Timing of Diagenetic Hematite Growth in Red Pelagic Limestones from Gubbio (Italy). Earth and Planetary Science Letters 58 (2), 189–201. https://doi.org/10.1016/0012-821X(82)90193-5.

Coccioni, R., 2020. Revised upper Barremian–upper Aptian planktonic foraminiferal biostratigraphy of the Gorgo a Cerbara section (central Italy). Newsletters on Stratigraphy 53, 275–295. https://doi.org/10.1127/nos/2019/0539.

Coccioni, R., 2022. In: Carta geologica con itinerari escursionistici, scala 1:20.000. Nuova edizione. Ente Parco Regionale del Conero, Sirolo (AN).

Coccioni, R., Premoli Silva, I., 2015. Revised upper Albian–Maastrichtian calcareous plankton biostratigraphy and magneto-stratigraphy of the classical Tethyan Gubbio section (Italy). Newsletters on Stratigraphy 48, 47–90. https://doi.org/10.1127/nos/2015/0055.

Coccioni, R., Franchi, R., Nesci, O., Wezel, F.C., Battistini, F., Pallecchi, P., 1989. Stratigraphy and mineralogy of the Selli level (early Aptian) at the base of the Marne a Fucoidi in the Umbro-Marchean Apennines (Italy). In: Weidmann, J. (Ed.), Cretaceous of the Western Tethys. E. Schweizerbart'sche Verlagsbuchhandlung, Stuttgart, Germany, pp. 563–584.

Coccioni, R., Montanari, A., Boschi, S., Catanzariti, R., Frontalini, F., Jovane, L., Kochhann, M.V.L., Pelosi, N., Sabatino, N., Savian, J.F., Sprovieri, M., 2022. Integrated stratigraphy of the Lutetian–Priabonian pelagic section at Bottaccione (Gubbio, central Italy): A proposal for defining and positioning the Global Stratotype Section and Point (GSSP) for the base of the Bartonian Stage (Paleogene System, Eocene Series). In: Koeberl, C., Claeys, P., Montanari, A. (Eds.), From the Guajira Desert to the Apennines, and from Mediterranean Microplates to the Mexican Killer Asteroid: Honoring the Career of Walter Alvarez, vol. 557. Geological Society of America Special Paper, pp. 311–346. https://doi.org/10.1130/2022.2557(16).

Coccioni, R., Moretti, E., Nesci, O., Savelli, D., Tramontana, M., Veneri, F., Wezel, F.C., 1994. Guide Geologiche Regionali. 15 Itinerari, Appennino umbro-marchigiano. Società Geologica Italiana, BE-MA, Milano, pp. 207–218.

Coccioni, R., Nesci, O., Tramontana, M., Wezel, F.C., Moretti, E., 1987. Descrizione di un livello-guida “radiolaritico-bituminoso-ittiolitico” alla base delle Marne a Fucoidi nell'Appennino umbro-marchigiano. Bollettino della Societa Geologica Italiana 106, 183–192.

Comune di Ancona, 2019. Ordinanza Sindacale n. 41/2019, Prot. Gen. n. 81031, 17/05/2019 “… divieto di accesso e stazionamento in quattro tratti di costa individuali nel litorale compreso tra lo "scoglio del Trave" e lo "scoglio della Vela" (limite del territorio comunale in direzione sud-est., pp. 1–12.

Cornamusini, G., Lazzarotto, A., Merlini, S., Pascucci, V., 2002. Eocene-Miocene evolution of the north Tyrrhenian Sea. Bollettino della Societa Geologica Italiana 1, 769–787.

Danilov, I.G., Obraztsova, E.M., Arkhangelsky, M.S., Ivanov, A.V., Averianov, A.O., 2022. *Protostega gigas* and other sea turtles from the Campanian of Eastern Europe, Russia. Cretaceous Research 135, 1–7. https://doi.org/10.1016/j.cretres.2022.105196.

D'Argenio, B., 1970. Evoluzione geottettonica comparata tra alcune piattaforme carbonatiche dei Mediterranei Europeo ed Americano. Atti Accademia Pontiana 20, 3–34.

Dewey, J.F., Pitman III, W.C., Ryan, W.B.F., Bonnin, J., 1973. Plate tectonics and the evolution of the alpine system. Geological Society of America Bulletin 84, 3137–3180.

Dunlop, D.J., Özdemir, Ö., 1997. Rock Magnetism: Fundamentals and Frontiers. Cambridge University Press.

Fisher, R.A., 1953. Dispersion on a sphere. Proceedings of the Royal Society of London A217, 295–305. https://doi.org/10.1098/rspa.1953.0064.

Frontalini, F., Rostami, M.A., Coccioni, R., 2016. Paleobathymetric assessments of the upper Albian–lower Danian Gubbio section (Italy). In: Menichetti, M., Coccioni, R., Montanari, S. (Eds.), The Stratigraphic Record of Gubbio: Integrated Stratigraphy of the Late Cretaceous/Paleogene Umbria Marche Pelagic Basin, vol 524. Geological Society of America Special Paper, pp. 105–113. https://doi.org/10.1130/2016.2524(08.

Gale, A., Batenburg, S., Coccioni, R., Zofia Dubicka, Z., Elisabetta Erba, E., et al., 2023. The Global Boundary Stratotype Section and Point (GSSP) of the Campanian Stage at Bottaccione (Gubbio, Italy) and its Auxiliary Sections: Seaford Head (UK), Bocieniec (Poland), Postalm (Austria), Smoky Hill, Kansas (U.S.A), Tepayac (Mexico). Episodes: Communications of IUGS Geological Standards 1–40. https://doi.org/10.18814/epiiugs/2022/022048.

Gardin, S., Galbrun, B., Thibault, N., Coccioni, R., Premoli Silva, I., 2012. Bio-magnetostratigraphy for the upper Campanian–Maastrichtian from the Gubbio area, Italy: New results from the Contessa Highway and Bottaccione sections.

Newsletters on Stratigraphy 45, 75–103. https://doi.org/10.1127/0078-0421/2012/0014.
Gibson, T.G., 1989. Planktonic benthonic foraminiferal ratios: Modern patterns and Tertiary applicability. Marine Micropaleontology 15, 29–52. https://doi.org/10.1016/0377-8398(89)90003-0.
Goatley, C.H.R., Hoey, A.S., Bellwood, D.R., 2012. The Role of Turtles as Coral Reef Macroherbivores. PLoS One 7 (6), e39979. https://doi.org/10.1371/journal.pone.0039979.
Gonzato, G., Ferrari, A.M., 2020. Le "Dropstone" nelle formazioni dei Monti Lessini. La Lessinia - Ieri Oggi Domani 43, 51–58. La Grafica, Verona.
Gradstein, F.M., Ogg, J.G., Schmitz, M.D., Ogg, G.M., 2020. The Cretaceous Period. Geologic Time Scale. Elsevier 2, 1023, 2020.
Huber, B.T., Petrizzo, M.R., Young, J.R., Falzoni, F., Gilardoni, S.E., Bown, P.R., Wade, B.S., 2016. Pforams@microtex: A new online taxonomic database for planktonic foraminifera. Micropaleontology 62, 429–438.
Husson, D., Galbrun, B., Gardin, S., Thibault, N., 2014. Tempo and duration of short-term environmental perturbations across the Cretaceous-Paleogene boundary. Stratigraphy 11, 159–171.
Kirschvink, J.L., 1980. The least-squares line and plane and the analysis of palaeomagnetic data. Geophysical Journal International 62 (3), 699–718. https://doi.org/10.1111/j.1365-246X.1980.tb02601.x.
Kuhnt, W., 1990. Agglutinated forams of western Mediterranean Upper Cretaceous pelagic limestones, Umbrian Apennines, Italy and Betic Cordillera, Spain. Micropaleontology 36, 297–330.
Lindgren, J., Caldwell, M.W., Konishi, T., Chiappe, L.M., 2010. Convergent Evolution in Aquatic Tetrapods: Insights from an Exceptional Fossil Mosasaur. Proceedings of the National Academy of Sciences 5 (8), 1–18. https://doi.org/10.1371/journal.pone.0011998.
Lirer, F., 2000. A new technique for retrieving calcareous microfossils from lithified lime deposits. Micropaleontology 46, 365–369.
Lockley, M.G., Cawthra, H.C., De Vynck, J.C., Helm, C.W., McCrea, R.T., Nele, R., 2019. New fossil sea turtle trackway morphotypes from the Pleistocene of South Africa highlight role of ichnology in turtle paleobiology. Quaternary Research 1–15. https://doi.org/10.1017/qua.2019.40.
Lockley, M.G., Smith, J.A., King, M.R., 2018. First reports of turtle tracks from the Williams Fork Formation ('Mesaverde' Group), Upper Cretaceous (Campanian) of western Colorado. Cretaceous Research 84, 474–482. https://doi.org/10.1016/j.cretres.2017.11.001.
Lowrie, W., Alvarez, W., 1976. Paleomagnetic studies of the Scaglia Rossa limestone in Umbria. Memorie della Societa Geologica Italiana 15, 41–50.
Lowrie, W., Alvarez, W., 1977. Late Cretaceous geomagnetic polarity sequence: detailed rock and palaeomagnetic studies of the Scaglia Rossa limestone at Gubbio, Italy. Geophysical Journal International 51 (3), 561–581. https://doi.org/10.1111/j.1365-246X.1977.tb04207.x.
Lowrie, W., 1990. Identification of ferromagnetic minerals in a rock by coercivity and unblocking temperature properties. Geophysical Research Letters 17, 159–162.
Lowrie, W., Alvarez, W., Asaro, F., 1990. The origin of the White Beds below the Cretaceous-Tertiary boundary in the Gubbio section, Italy. Earth and Planetary Science Letters 98, 303–312. https://doi.org/10.1016/0012-821X(90)90032-S.
Lurcock, P.C., Wilson, G.S., 2012. PuffinPlot: A versatile, user-friendly program for paleomagnetic analysis. Geochemistry, Geophysics, Geosystems 13, Q06Z45. https://doi.org/10.1029/2012GC004098.
Marroni, M., Molli, G., Ottria, G., Pandolfi, L., 2001. Tectono-sedimentary evolution of the External Liguride units (Northern Apennines, Italy): Insights in the pre-collisional history of a fossil ocean-continent transition zone. Geodinamica Acta 14, 307–320. https://doi.org/10.1080/09853111.2001.11432449.
Miniati, F., Petrizzo, M.R., Falzoni, F., Erba, E., 2020. Calcareous plankton biostratigraphy of the Santonian-Campanian boundary interval in the Bottaccione section (Umbria-Marche Basin, central Italy). Rivista Italiana di Paleontologia e Stratigrafia 126 (3), 771–789.
Montanari, A., 1979. Lineamenti Sedimentologici della "Scaglia Bianca" e della "Scaglia Rossa" nelle Marche Settentrionali. University of Urbino, Urbino, Italy, pp. 1–289 [Laurea thesis].
Montanari, A., 1988. Tectonic implications of hydrothermal mineralization in the late Cretaceous-early Tertiary pelagic basin of the northern Apennines. Bollettino della Societa Geologica Italiana 107, 399–411.
Montanari, A., Koeberl, C., 2000. Impact Stratigraphy: The Italian Record. Lecture Notes in Earth Sciences 93, 1–364. Berlin Heidelberg, Springer-Verlag.
Montanari, A., Chan, L.S., Alvarez, W., 1989. Synsedimentary tectonics in the Late Cretaceous–early Tertiary pelagic basin of the Northern Apennines. In: Crevello, P.D., Wilson, J.L., Sarg, J.F., Read, J.F. (Eds.), Controls on Carbonate Platform and Basin Development, vol. 44. Society for Sedimentary Geology (SEPM) Special Publication, pp. 379–399. https://doi.org/10.2110/pec.89.44.0379.
Montanari, A., Mainiero, M., Coccioni, R., Pignocchi, G., 2016. Catastrophic landslide of Medieval Portonovo (Ancona, Italy). Geological Society of America Bulletin 118, 1660–1678.
Montanari, A., Farley, K., Coccioni, R., Sabatino, N., Bice, D., Yesko, M., Sinnesael, M., deWinter, N., 2023. Cosmogenic 3He anomaly K1 vs. the early Campanian isotopic event (ECE) as recorded in pelagic limestones of the Umbria-Marche succession (Italy). Geological Society of America Bulletin 136, 1753–1767.
Mukhopadhyay, S., Farley, K.A., Montanari, A., 2001. A short duration of the Cretaceous-Tertiary boundary event: Evidence from extraterrestrial helium-3. Science 291 (5510), 1952–1955. https://doi.org/10.1126/science.291.5510.1952.
Natali, L., Leonardi, G., 2023. *Coneroichnus marinus* ichnogenus et ichnospecies nov., a fossil trackway of marine reptile in the Maiolica Formation (Upper Jurassic-Lower Cretaceous) from Mount Conero, Marche, Italy. Revista Brasileira de Paleontologia 26 (3), 156–171. https://doi.org/10.4072/rbp.2023.3.02.
Natali, L., Blasetti, A., Crocetti, G., 2019. Detection of lower Cretaceous fossil impressions of a marine reptile on Monte Conero (Central Italy). Cretaceous Research 93, 143–150. https://doi.org/10.1016/j.cretres.2018.09.014.
Nyong, E.E., Olsson, R.K., 1984. A paleoslope model of Campanian to lower Maestrichtian foraminifera in the North American basin and adjacent continental margin. Marine Micropaleontology 8, 437–477. https://doi.org/10.1016/0377-8398(84)90009-4.
Olsson, R.K., Nyong, E.E., 1984. A paleoslope model for Campanian–lower Maastrichtian foraminifera of New Jersey and Delaware. Journal of Foraminiferal Research 14, 50–68. https://doi.org/10.2113/gsjfr.14.1.50.
Rochette, P., Mathé, P.-E., Esteban, L., Rakoto, H., Bouchez, J.-L., Liu, Q., Torrent, J., 2005. Non-saturation of the defect moment of goethite and fine-grained hematite up to 57 Teslas. Geophysical Research Letters 32, L22309. https://doi.org/10.1029/2005GL024196.
Sabatino, N., Meyers, S.R., Voigt, S., Coccioni, R., Sprovieri, M., 2018. A new high-resolution carbon- carbon-isotope stratigraphy for the Campanian (Bottaccione section): Its implications for global correlation, ocean circulation, and astrochronology. Palaeogeography, Palaeoclimatology, Palaeoecology 489, 29–39. https://doi.org/10.1016/j.palaeo.2017.08.026.
Serafini, G., Gordon, C., Amalfitano, J., Wings, O., Esteban, N., Stokes, H., Giusberti, L., 2024. First evidence of marine turtle gastroliths in a fossil specimen: Paleobiological implications in comparison to modern analogues. PLoS One 19, 1–28.
Sinnesael, M., De Vleeschouwer, D., Coccioni, R., Claeys, P., Frontalini, F., Jovane, L., Savian, J.F., Montanari, A., 2016. High-resolution multiproxy cyclostratigraphic analysis of environmental and climatic events across the Cretaceous-Paleogene boundary in the classic pelagic succession of Gubbio (Italy). In: Menichetti, M., Coccioni, R., Montanari, A. (Eds.), The Stratigraphic Record of Gubbio: Integrated Stratigraphy of the Late Cretaceous–Paleogene Umbria-Marche Pelagic Basin, vol 524. Geological Society of America Special Paper, pp. 115–137. https://doi.org/10.1130/2016.2524(09.
Sliter, W.V., Baker, A., 1972. Cretaceous bathymetric distribution of benthic foraminifera. Journal of Foraminiferal Research 2, 167–183. https://doi.org/10.2113/gsjfr.2.4.167.
Tjalsma, R.C., Lohmann, G.P., 1983. Paleocene–Eocene bathyal and abyssal benthic foraminifera from the Atlantic Ocean. Micropaleontology Special Publication 4, 90.
Treves, B., 1984. Orogenic belts as accretionary prisms: The example of the Northern Apennines. Ofioliti 9, 577–618.
van der Zwaan, G.J., Jorissen, F.J., Stigter, H.C., 1990. The depth dependency of planktonic/benthic foraminiferal ratios: Constraints and applications. Marine Geology 95, 1–16. https://doi.org/10.1016/0025-3227(90)90016-D.
van Morkhoven, F.P.C.M., Berggren, W.A., Edwards, A.S., 1986. Cenozoic cosmopolitan deep-water benthic foraminifera. Bulletin des Centres de Recherches Exploration-Production Elf-Aquitaine Mémoire 11, 421. https://doi.org/10.2113/gsjfr.18.1.90.
Wendler, I., 2013. A critical evaluation of carbon isotope stratigraphy and biostratigraphic implications for Late Cretaceous global correlation. Earth-Science Reviews 126, 116–146. https://doi.org/10.1016/j.earscirev.2013.08.003.
Wibbels, T., Bevan, E., 2016. A Historical Perspective of the Biology and Conservation of the Kemp's Ridley Sea Turtle. Gulf of Mexico Science 2, 129–137. https://doi.org/10.18785/goms.3302.02.
Widmark, J.G.V., 1997. Deep-sea benthic foraminifera from Cretaceous-Paleogene boundary strata in the South Atlantic-Taxonomy and paleoecology. Fossils and Strata 43, 1–94.
Widmark, J.G.V., Speijer, R.P., 1997. Benthic Foraminiferal Faunas and Trophic Regimes at the Terminal Cretaceous Tethyan Seafloor. PALAIOS 12, 354–371. https://doi.org/10.2307/3515335.
Zhang, Q., Wen, W., Hu, S., Benton, M.J., Zhou, C., et al., 2014. Nothosaur foraging tracks from the Middle Triassic of southwestern China. Nature Communications 5 (3973), 1–12. https://doi.org/10.1038/ncomms4973.
Zorzin, R., 2016. Rocce e fossili del Monte Baldo e dei Monti Lessini Veronesi. Cierre Edizioni, Sommacampagna (Verona) 176.
Zorzin, R., 2017. In: Vertebrati fossili marini e terrestri del Veronese. Cierre Edizioni, Caselle di Sommacampagna (Verona), p. 176.
Zorzin, R., 2022. In: Fossili e rocce del Veronese. Cierre Edizioni, Caselle di Sommacampagna (Verona), p. 223.

Appendix A. Supplementary data

Supplementary data to this article can be found online at https://doi.org/10.1016/j.cretres.2025.106268.